
FedSKETCH: Communication-Efficient Federated Learning via Sketching

Anonymous Author(s)

Affiliation

Address

email

Abstract

1 Communication complexity and data privacy are the two key challenges in Federated Learning (FL) where the goal is to perform a distributed learning through a
2 large volume of devices. In this work, we introduce two new algorithms, namely
3 FedSKETCH and FedSKETCHGATE, to address jointly both challenges and which
4 are, respectively, intended to be used for homogeneous and heterogeneous data distribution settings. Our algorithms are based on a key and novel sketching technique,
5 called HEAPRIX that is unbiased, compresses the accumulation of local gradients
6 using count sketch, and exhibits communication-efficiency properties leveraging
7 low-dimensional sketches. We provide sharp convergence guarantees of our
8 algorithms and validate our theoretical findings with various sets of experiments.
9
10

1 Introduction

12 Federated Learning (FL) is a recently emerging framework for distributed large scale machine
13 learning problems. In FL, data is distributed across devices [33; 23] and due to privacy concerns,
14 users are only allowed to communicate with the parameter server. Formally, the optimization problem
15 across p distributed devices is defined as follows:

$$\min_{\mathbf{x} \in \mathbb{R}^d, \sum_{j=1}^p q_j = 1} f(\mathbf{x}) \triangleq \sum_{j=1}^p q_j F_j(\mathbf{x}), \quad (1)$$

16 where $F_j(\mathbf{x}) = \mathbb{E}_{\xi \in \mathcal{D}_j} [L_j(\mathbf{x}, \xi)]$ is the local cost function at device j , $q_j \triangleq \frac{n_j}{n}$, n_j is the number
17 of data shards at device j and $n = \sum_{j=1}^p n_j$ is the total number of data samples, ξ is a random
18 variable distributed according to probability distribution \mathcal{D}_j , and L_j is a loss function that measures
19 the performance of model \mathbf{x} at device j . We note that, while for the homogeneous setting we
20 assume $\{\mathcal{D}_j\}_{j=1}^p$ have the same distribution across devices and $L_i = L_j$, $1 \leq (i, j) \leq p$, in the
21 heterogeneous setting, these distributions and loss functions L_j can vary from a device to another.

22 There are several challenges that need to be addressed in FL in order to efficiently learn a global
23 model that performs well in average for all devices:

24 – *Communication-efficiency*: There are often many devices communicating with the server, thus
25 incurring immense communication overhead. One approach to reduce communication round is using
26 *local SGD with periodic averaging* [48; 41; 47; 43] which periodically averages models after few
27 local updates, contrary to baseline SGD [6] where model averaging is performed at each iteration.
28 Local SGD has been proposed in McMahan et al. [33]; Konečný et al. [23] under the FL setting and
29 its convergence analysis is studied in Stich [41]; Wang and Joshi [43]; Zhou and Cong [48]; Yu et al.
30 [47], later on improved in the follow up references [3; 12; 21; 39] for homogeneous setting. It is
31 further extended to heterogeneous setting [46; 30; 38; 31; 12; 20]. Second approach to deal with
32 communication cost aims at reducing the size of communicated message per communication round,
33 such as local gradient quantization [1; 4; 42; 44; 45] or sparsification [2; 32; 40; 39].

34 *–Data heterogeneity:* Since locally generated data in each device may come from different distribution,
 35 local computations involved in FL setting can lead to poor convergence error in practice [27; 31].
 36 To mitigate the negative impact of data heterogeneity, [13; 16; 31; 20] suggest applying variance
 37 reduction or gradient tracking techniques along local computations.

38 *–Privacy* [11; 14]: Privacy has been widely addressed by injecting an additional layer of randomness
 39 to respect differential-privacy property [34] or using cryptography-based approaches under secure
 40 multi-party computation [5]. Further study of challenges can be found in recent surveys [28] and [18].

41 To tackle all major aforementioned challenges in FL jointly, sketching based algorithms [7; 9; 22; 25]
 42 are promising approaches. For instance, to reduce communication cost, [17] develop a distributed
 43 SGD algorithm using sketching along providing its convergence analysis in the homogeneous setting,
 44 and establish a communication complexity of order $\mathcal{O}(\log(d))$ per round, where d is the dimension
 45 of the vector of parameters compared to $\mathcal{O}(d)$ complexity per round of baseline mini-batch SGD. Yet,
 46 the proposed sketching scheme in Ivkin et al. [17], built from a communication-efficiency perspective,
 47 is based on a deterministic procedure which requires access to the exact information of the gradients,
 48 thus not meeting the crucial privacy-preserving criteria. This systemic flaw is partially addressed
 49 in Rothchild et al. [37].

50 Focusing on privacy, [26] derive a single framework in order to tackle these issues jointly and
 51 introduces DiffSketch algorithm, based on the Count Sketch operator, yet does not provide its
 52 convergence analysis. Additionally, the estimation error of DiffSketch is higher than the sketching
 53 scheme in Ivkin et al. [17] which may end up in poor convergence.

54 In this paper, we propose new sketching algorithms to address the aforementioned challenges
 55 simultaneously. Our main contributions are summarized as:

- 56 • We provide a new algorithm – HEAPRIX – and theoretically show that it reduces the cost
 57 of communication between devices and server, which is based on unbiased sketching with-
 58 out requiring the broadcast of exact values of gradients to the server. Based on HEAPRIX,
 59 we develop general algorithms for communication-efficient and sketch-based FL, namely
 60 FedSKETCH and FedSKETCHGATE for both homogeneous and heterogeneous data distribu-
 61 tion settings respectively.
- 62 • We establish non-asymptotic convergence bounds for convex, Polyak-Łojasiewicz (PL) and
 63 non-convex functions in Theorems 1 and 2 in both homogeneous and heterogeneous cases,
 64 and highlight an improvement in the number of iteration to reach a stationary point. We also
 65 provide a convergence analysis for the PRIVIX algorithm proposed in Li et al. [26].
- 66 • We illustrate the benefits of FedSKETCH and FedSKETCHGATE over baseline methods through
 67 a set of experiments. The latter shows the advantages of the HEAPRIX compression method
 68 achieving comparable test accuracy as Federated SGD (FedSGD) while compressing the
 69 information exchanged between devices and server.

70 **Notation:** We denote the number of communication rounds and bits per round and per device by
 71 R and B respectively. The count sketch of any vector \mathbf{x} is designated by $\mathbf{S}(\mathbf{x})$. $[p]$ denotes the set
 72 $\{1, \dots, p\}$.

73 2 Compression using Count Sketch

74 In this paper, we exploit the commonly used Count Sketch [7] which uses two sets of functions
 75 that encode any input vector \mathbf{x} into a hash table $\mathbf{S}_{m \times t}(\mathbf{x})$. Pairwise independent hash functions
 76 $\{h_{j,1 \leq j \leq t} : [d] \rightarrow [m]\}$ are used along with another set of pairwise independent sign hash functions
 77 $\{\text{sign}_{j,1 \leq j \leq t} : [d] \rightarrow \{+1, -1\}\}$ to map entries of \mathbf{x} ($x_i, 1 \leq i \leq d$) into t different columns of
 78 $\mathbf{S}_{m \times t}$, wherein to lower the dimension of the input vector we usually have $d \gg mt$. The final update
 79 reads $\mathbf{S}[j][h_j(i)] = \mathbf{S}[j-1][h_{j-1}(i)] + \text{sign}_j(i) \cdot x_i$ for any $1 \leq j \leq t$. There are various types of
 80 sketching algorithms which are developed based on count sketching that we develop in the following
 81 subsections. See the Appendix for the detailed Count Sketch algorithm.

82 2.1 Sketching based Unbiased Compressor

83 We define an unbiased compressor as follows:

84 **Definition 1** (Unbiased compressor). A randomized function, $C : \mathbb{R}^d \rightarrow \mathbb{R}^d$ is called an unbiased
 85 compression operator with $\Delta \geq 1$, if we have

$$\mathbb{E}[C(\mathbf{x})] = \mathbf{x} \quad \text{and} \quad \mathbb{E}[\|C(\mathbf{x})\|_2^2] \leq \Delta \|\mathbf{x}\|_2^2.$$

86 We denote this class of compressors by $\mathbb{U}(\Delta)$.

87 This definition leads to the following property

$$\mathbb{E}[\|C(\mathbf{x}) - \mathbf{x}\|_2^2] \leq (\Delta - 1) \|\mathbf{x}\|_2^2.$$

88 Note that if we let $\Delta = 1$ then our algorithm reduces to the case of no compression. This property
 89 allows us to control the noise of the compression.

90 An instance of such unbiased compressor is PRIVIX which obtains an estimate of input \mathbf{x} from a
 91 count sketch noted $\mathbf{S}(\mathbf{x})$. In this algorithm, to query the quantity x_i , the i -th element of the vector
 92 \mathbf{x} , we compute the median of t approximated values specified by the indices of $h_j(i)$ for $1 \leq j \leq t$,
 93 see [26] or Algorithm 6 in the Appendix (for more details). For the purpose of our proof, we state the
 94 following crucial properties of the count sketch:

95 **Property 1** (Li et al. [26]). For any $\mathbf{x} \in \mathbb{R}^d$, we have:

96 *Unbiased estimation:* As in Li et al. [26], we have:

$$\mathbb{E}_{\mathbf{S}}[\text{PRIVIX}[\mathbf{S}(\mathbf{x})]] = \mathbf{x}.$$

97 *Bounded variance:* For the given $m < d$, $t = \mathcal{O}(\ln(\frac{d}{\delta}))$ with probability $1 - \delta$ we have:

$$\mathbb{E}_{\mathbf{S}}[\|\text{PRIVIX}[\mathbf{S}(\mathbf{x})] - \mathbf{x}\|_2^2] \leq c \frac{d}{m} \|\mathbf{x}\|_2^2,$$

98 where c ($e \leq c < m$) is a positive constant independent of the dimension of the input, d .

99 Thus, with probability $1 - \delta$ we obtain that $\text{PRIVIX} \in \mathbb{U}(1 + c \frac{d}{m})$. Note $\Delta = 1 + c \frac{d}{m}$ implies that if
 100 $m \rightarrow d$, then $\Delta \rightarrow 1 + c$, indicating a noisy reconstruction. Exploiting this noisy reconstruction, Li
 101 et al. [26] show that if the data is normally distributed, PRIVIX is differentially private [10], up to
 102 additional assumptions and algorithmic design.

103 2.2 Sketching based Biased Compressor

104 A biased compressor is defined as follows:

105 **Definition 2** (Biased compressor). A (randomized) function, $C : \mathbb{R}^d \rightarrow \mathbb{R}^d$ belongs to $\mathbb{C}(\Delta, \alpha)$, a
 106 class of compression operators with $\alpha > 0$ and $\Delta \geq 1$, if

$$\mathbb{E}[\|\alpha \mathbf{x} - C(\mathbf{x})\|_2^2] \leq \left(1 - \frac{1}{\Delta}\right) \|\mathbf{x}\|_2^2,$$

107 The reference [15] proves that $\mathbb{U}(\Delta) \subset \mathbb{C}(\Delta, \alpha)$. An example of biased compression via sketching
 108 and using top_m operation is given below:

Algorithm 1 HEAVYMIX

- 1: **Inputs:** $\mathbf{S}(\mathbf{g})$; parameter m
 - 2: Query the vector $\tilde{\mathbf{g}} \in \mathbb{R}^d$ from $\mathbf{S}(\mathbf{g})$:
 - 3: Query $\hat{\ell}_2^2 = (1 \pm 0.5) \|\mathbf{g}\|^2$ from sketch $\mathbf{S}(\mathbf{g})$
 - 4: $\forall j$ query $\hat{\mathbf{g}}_j^2 = \tilde{\mathbf{g}}_j^2 \pm \frac{1}{2m} \|\mathbf{g}\|^2$ from sketch $\mathbf{S}(\mathbf{g})$
 - 5: $H = \{j | \hat{\mathbf{g}}_j^2 \geq \frac{\hat{\ell}_2^2}{m}\}$ and $NH = \{j | \hat{\mathbf{g}}_j^2 < \frac{\hat{\ell}_2^2}{m}\}$
 - 6: $\text{Top}_m = H \cup \text{rand}_{\ell}(NH)$, where $\ell = m - |H|$
 - 7: Get exact values of Top_m
 - 8: **Output:** $\tilde{\mathbf{g}} : \forall j \in \text{Top}_m : \tilde{\mathbf{g}}_j = \mathbf{g}_j$ else $\mathbf{g}_j = 0$
-

109 Following Ivkin et al. [17], HEAVYMIX with sketch size $\Theta(m \log(\frac{d}{\delta}))$ is a biased compressor
 110 with $\alpha = 1$ and $\Delta = d/m$ with probability $\geq 1 - \delta$. In other words, with probability $1 - \delta$,

111 HEAVYMIX $\in C(\frac{d}{m}, 1)$. We note that Algorithm 1 is a variation of the sketching algorithm developed
 112 in Ivkin et al. [17] with distinction that HEAVYMIX does not require a second round of communication
 113 to obtain the exact values of top_m . Additionally, while a sketching algorithm implementing HEAVYMIX
 114 has smaller estimation error compared to PRIVIX, it requires having access to the exact values of
 115 top_m , therefore not benefiting from privacy properties contrary to PRIVIX. In the following we
 116 introduce our sketching scheme – HEAPRIX – as a combination of those two methods.

117 2.3 Sketching based Induced Compressor

118 Due to Theorem 3 in Horváth and Richtárik [15], which illustrates that we can convert the biased
 119 compressor into an unbiased one such that, for $C_1 \in \mathbb{C}(\Delta_1)$ with $\alpha = 1$, if you choose $C_2 \in \mathbb{U}(\Delta_2)$,
 120 then induced compressor $C : x \mapsto C_1(x) + C_2(x - C_1(x))$ belongs to $\mathbb{U}(\Delta)$ with $\Delta = \Delta_2 + \frac{1-\Delta_2}{\Delta_1}$.
 121 Based on this notion, Algorithm 2 proposes an induced sketching algorithm by utilizing HEAVYMIX
 122 and PRIVIX for C_1 and C_2 respectively where the reconstruction of input x is performed using hash
 123 table \mathbf{S} and x , similar to PRIVIX and HEAVYMIX.

Algorithm 2 HEAPRIX

- 1: **Inputs:** $x \in \mathbb{R}^d, t, m, \mathbf{S}_{m \times t}, h_j(1 \leq i \leq t), \text{sign}_j(1 \leq i \leq t)$, parameter m
 - 2: Approximate $\mathbf{S}(x)$ using HEAVYMIX
 - 3: Approximate $\mathbf{S}(x - \text{HEAVYMIX}[\mathbf{S}(x)])$ using PRIVIX
 - 4: **Output:**

$$\text{HEAVYMIX}[\mathbf{S}(x)] + \text{PRIVIX}[\mathbf{S}(x - \text{HEAVYMIX}[\mathbf{S}(x)])]$$
-

124 Note that if $m \rightarrow d$, then $C(x) \rightarrow x$, which implies that the convergence rate of the algorithm can
 125 be improved by decreasing the size of compression m .

126 **Corollary 1.** *Based on Theorem 3 of [15], HEAPRIX in Algorithm 2 satisfies $C(x) \in \mathbb{U}(c\frac{d}{m})$.*

127 *Benefits of HEAPRIX:* Corollary 1 states that, unlike PRIVIX, HEAPRIX compression noise can be
 128 made as small as possible using larger hash size. Contrary to HEAVYMIX, HEAPRIX does not require
 129 having access to exact top_m values of the input, thus helps preserving privacy. In other words,
 130 HEAPRIX leverages the best of both worlds: the *unbiasedness* of PRIVIX while using *heavy hitters* as
 131 in HEAVYMIX.

132 3 FedSKETCH and FedSKETCHGATE

133 We define two general frameworks for different sketching algorithms for homogeneous and heteroge-
 134 neous settings.

135 3.1 Homogeneous Setting

136 In FedSKETCH, the number of local updates, between two consecutive communication rounds, at
 137 device j is denoted by τ . Unlike Haddadpour et al. [13], server node does not store any global model,
 138 rather, device j has two models: $x^{(r)}$ and $x_j^{(\ell, r)}$, which are respectively the local and global models.
 139 We develop FedSKETCH in Algorithm 3. A variant of this algorithm implementing HEAPRIX is also
 140 described in Algorithm 3. We note that for this variant, we need to have an additional communication
 141 round between server and worker j to aggregate $\delta_j^{(r)} \triangleq \mathbf{S}_j[\text{HEAVYMIX}(\mathbf{S}^{(r)})]$, see Lines 3 and 3.
 142 The main difference between our FedSKETCH and the DiffSketch algorithm in Li et al. [26] is that
 143 we use distinct local and global learning rates. Furthermore, unlike Li et al. [26], we do not add local
 144 Gaussian noise.

145 **Algorithmic comparison with Haddadpour et al. [13]** An important feature of our algorithm is that
 146 due to a lower dimension of the count sketch, the resulting averages ($\mathbf{S}^{(r)}$ and $\tilde{\mathbf{S}}^{(r)}$) received by the
 147 server, are also of lower dimension. Therefore, these algorithms exploit a bidirectional compression
 148 during the communication from server to device back and forth. As a result, due to this bidirectional
 149 property of communicating sketching for the case of large quantization error $\omega = \theta(\frac{d}{m})$ as shown
 150 in Haddadpour et al. [13], our algorithms can outperform FedCOM and FedCOMGATE developed
 151 in Haddadpour et al. [13] if sufficiently large hash tables are used and the uplink communication cost
 152 is high. Furthermore, while, in Haddadpour et al. [13], server stores a global model and aggregates

Algorithm 3 FedSKETCH(R, τ, η, γ)

1: **Inputs:** $\mathbf{x}^{(0)}$: initial model shared by all local devices, global and local learning rates γ and η , respectively
2: **for** $r = 0, \dots, R - 1$ **do**
3: **parallel for device** $j \in \mathcal{K}^{(r)}$ **do**:
4: **if PRIVIX variant:**
$$\Phi^{(r)} \triangleq \text{PRIVIX} \left[\mathbf{S}^{(r-1)} \right]$$

5: **if HEAPRIX variant:**
$$\Phi^{(r)} \triangleq \text{HEAVYMIX} \left[\mathbf{S}^{(r-1)} \right] + \text{PRIVIX} \left[\mathbf{S}^{(r-1)} - \tilde{\mathbf{S}}^{(r-1)} \right]$$

6: Set $\mathbf{x}^{(r)} = \mathbf{x}^{(r-1)} - \gamma \Phi^{(r)}$ and $\mathbf{x}_j^{(0,r)} = \mathbf{x}^{(r)}$
7: **for** $\ell = 0, \dots, \tau - 1$ **do**
8: Sample a mini-batch $\xi_j^{(\ell,r)}$ and compute $\tilde{\mathbf{g}}_j^{(\ell,r)}$
9: Update $\mathbf{x}_j^{(\ell+1,r)} = \mathbf{x}_j^{(\ell,r)} - \eta \tilde{\mathbf{g}}_j^{(\ell,r)}$
10: **end for**
11: Device j broadcasts $\mathbf{S}_j^{(r)} \triangleq \mathbf{S}_j \left(\mathbf{x}_j^{(0,r)} - \mathbf{x}_j^{(\tau,r)} \right)$.
12: Server **computes** $\mathbf{S}^{(r)} = \frac{1}{k} \sum_{j \in \mathcal{K}} \mathbf{S}_j^{(r)}$.
13: Server **broadcasts** $\mathbf{S}^{(r)}$ to devices in randomly drawn devices $\mathcal{K}^{(r)}$.
14: **if HEAPRIX variant:**
15: Second round of communication: $\delta_j^{(r)} := \mathbf{S}_j \left[\text{HEAVYMIX}(\mathbf{S}^{(r)}) \right]$ and broadcasts $\tilde{\mathbf{S}}^{(r)} \triangleq \frac{1}{k} \sum_{j \in \mathcal{K}} \delta_j^{(r)}$ to devices in set $\mathcal{K}^{(r)}$
16: **end parallel for**
17: **end**
18: **Output:** $\mathbf{x}^{(R-1)}$

153 the partial gradients from devices which can enable the server to extract some information regarding
154 the device's data, in contrast, in our algorithms server does not store the global model and only
155 broadcasts the average sketches. Thus, sketching-based server-devices communication algorithms
156 such as ours do not reveal the exact values of the inputs, to preserve privacy as a by-product.

157 **Remark 1.** As pointed out in Horváth and Richtárik [15], while induced compressors transform a
158 biased compressor into unbiased one, as a drawback it doubles communication cost since the devices
159 need to send $C_1(\mathbf{x})$ and $C_2(\mathbf{x} - C_1(\mathbf{x}))$ separately. We note that in the special case of HEAPRIX,
160 due to the use of sketching, the extra communication round cost is compensated with lower number of
161 bits per round thanks to the lower dimension of sketching.

162 3.2 Heterogeneous Setting

163 In this section, we focus on the optimization problem of (1) in the special case of $q_1 = \dots = q_p = \frac{1}{p}$
164 with full device participation ($k = p$). These results can be extended to the scenario where devices
165 are sampled. For non i.i.d. data, the FedSKETCH algorithm, designed for homogeneous setting, may
166 fail to perform well in practice. The main reason is that in FL, devices are using local stochastic
167 descent direction which could be different than global descent direction when the data distribution are
168 non-identical. Therefore, to mitigate the effect of data heterogeneity, we introduce a new algorithm
169 called FedSKETCHGATE described in Algorithm 4. This algorithm leverages the idea of gradient
170 tracking applied in Haddadpour et al. [13] (with compression) and a special case of $\gamma = 1$ without
171 compression [31]. The main idea is that using an approximation of global gradient, $\mathbf{c}_j^{(r)}$ allows to
172 correct the local gradient direction. For the FedSKETCHGATE with PRIVIX variant, the correction
173 vector $\mathbf{c}_j^{(r)}$ at device j and communication round r is computed in Line 4. While using HEAPRIX
174 compression, FedSKETCHGATE also updates $\tilde{\mathbf{S}}^{(r)}$ via Line 4.

175 **Remark 2.** Most of the existing communication-efficient algorithms with compression only consider
176 communication-efficiency from devices to server. However, Algorithms 3 and 4 also improve the

Algorithm 4 FedSKETCHGATE(R, τ, η, γ)

1: **Inputs:** $\mathbf{x}^{(0)} = \mathbf{x}_j^{(0)}$ shared by all local devices, global and local learning rates γ and η .
2: **for** $r = 0, \dots, R - 1$ **do**
3: **parallel for device** $j = 1, \dots, p$ **do**
4: **if PRIVIX variant:**
$$\mathbf{c}_j^{(r)} = \mathbf{c}_j^{(r-1)} - \frac{1}{\tau} \left[\text{PRIVIX} \left(\mathbf{S}^{(r-1)} \right) - \text{PRIVIX} \left(\mathbf{S}_j^{(r-1)} \right) \right]$$

5: where $\Phi^{(r)} \triangleq \text{PRIVIX}(\mathbf{S}^{(r-1)})$
6: **if HEAPRIX variant:**
$$\mathbf{c}_j^{(r)} = \mathbf{c}_j^{(r-1)} - \frac{1}{\tau} \left(\Phi^{(r)} - \Phi_j^{(r)} \right)$$

7: Set $\mathbf{x}^{(r)} = \mathbf{x}^{(r-1)} - \gamma \Phi^{(r)}$ and $\mathbf{x}_j^{(0,r)} = \mathbf{x}^{(r)}$
8: **for** $\ell = 0, \dots, \tau - 1$ **do**
9: Sample mini-batch $\xi_j^{(\ell,r)}$ and compute $\tilde{\mathbf{g}}_j^{(\ell,r)}$
10: $\mathbf{x}_j^{(\ell+1,r)} = \mathbf{x}_j^{(\ell,r)} - \eta \left(\tilde{\mathbf{g}}_j^{(\ell,r)} - \mathbf{c}_j^{(r)} \right)$
11: **end for**
12: Device j broadcasts $\mathbf{S}_j^{(r)} \triangleq \mathbf{S} \left(\mathbf{x}_j^{(0,r)} - \mathbf{x}_j^{(\tau,r)} \right)$.
13: Server **computes** $\mathbf{S}^{(r)} = \frac{1}{p} \sum_{j=1}^p \mathbf{S}_j^{(r)}$ and **broadcasts** $\mathbf{S}^{(r)}$ to all devices.
14: **if HEAPRIX variant:**
15: Device j computes $\Phi_j^{(r)} \triangleq \text{HEAPRIX}[\mathbf{S}_j^{(r)}]$
16: Second round of communication to obtain $\delta_j^{(r)} := \mathbf{S}_j \left(\text{HEAVYMIX}[\mathbf{S}^{(r)}] \right)$
17: Broadcasts $\tilde{\mathbf{S}}^{(r)} \triangleq \frac{1}{p} \sum_{j=1}^p \delta_j^{(r)}$ to devices
18: **end parallel for**
19: **end**
20: **Output:** $\mathbf{x}^{(R-1)}$

177 *communication efficiency from server to devices since it exploits low-dimensional sketches (and*
178 *averages), communicated from the server to devices.*

179 For both FedSKETCH and FedSKETCHGATE algorithms, unlike PRIVIX, HEAPRIX variant requires
180 a second round of communication. Therefore, in Cross-Device FL setting, where there could be
181 millions of devices, HEAPRIX variant may not be practical, and we note that it could be more suitable
182 for Cross-Silo FL setting.

183 4 Convergence Analysis

184 We first state commonly used assumptions required in the following convergence analysis (reminder
185 of our notations can be found Table 1 of the Appendix).

186 **Assumption 1** (Smoothness and Lower Boundedness). *The local objective function $f_j(\cdot)$ of device*
187 *j is differentiable for $j \in [p]$ and L -smooth, i.e., $\|\nabla f_j(\mathbf{x}) - \nabla f_j(\mathbf{y})\| \leq L\|\mathbf{x} - \mathbf{y}\|$, $\forall \mathbf{x}, \mathbf{y} \in \mathbb{R}^d$.*
188 *Moreover, the optimal objective function $f(\cdot)$ is bounded below by $f^* := \min_{\mathbf{x}} f(\mathbf{x}) > -\infty$.*

189 Assumption 1 is common in stochastic optimization. We present our results for PL, convex and
190 general non-convex objectives. The reference [19] show that PL condition implies strong convexity
191 property with same module (PL objectives can also be non-convex, hence strong convexity does not
192 imply PL condition necessarily).

193 4.1 Convergence of FEDSKETCH

194 We now focus on the homogeneous case where data is i.i.d. among local devices, and therefore, the
195 stochastic local gradient of each worker is an unbiased estimator of the global gradient. We have:

196 **Assumption 2** (Bounded Variance). For all $j \in [m]$, we can sample an independent mini-batch
 197 ℓ_j of size $|\Xi_j^{(\ell,r)}| = b$ and compute an unbiased stochastic gradient $\tilde{\mathbf{g}}_j = \nabla f_j(\mathbf{x}; \Xi_j)$, $\mathbb{E}_{\Xi_j}[\tilde{\mathbf{g}}_j] =$
 198 $\nabla f(\mathbf{x}) = \mathbf{g}$ with the variance bounded is bounded by a constant σ^2 , i.e., $\mathbb{E}_{\Xi_j}[\|\tilde{\mathbf{g}}_j - \mathbf{g}\|^2] \leq \sigma^2$.

199 **Theorem 1.** Suppose Assumptions 1-2 hold. Given $0 < m \leq d$ and considering Algorithm 3 with
 200 sketch size $B = O(m \log(\frac{dR}{\delta}))$ and $\gamma \geq k$, with probability $1 - \delta$ we have: In the **non-convex**
 201 case, $\{\mathbf{x}^{(r)}\}_{r=0}^R$ satisfies $\frac{1}{R} \sum_{r=0}^{R-1} \|\nabla f(\mathbf{x}^{(r)})\|_2^2 \leq \epsilon$ if:

202 • **FS-PRIVIX**, for $\eta = \frac{1}{L\gamma} \sqrt{\frac{k}{R\tau(\frac{cd}{mk}+1)}}$:

$$R = O(1/\epsilon) \quad \text{and} \quad \tau = O((d+m)/(mk\epsilon)) .$$

203 • **FS-HEAPRIX**, for $\eta = \frac{1}{L\gamma} \sqrt{\frac{k}{R\tau(\frac{cd-m}{mk}+1)}}$:

$$R = O(1/\epsilon) \quad \text{and} \quad \tau = O(d/(mk\epsilon)) .$$

204 In the **PL or strongly convex** case, $\{\mathbf{x}^{(r)}\}_{r=0}^R$ satisfies $\mathbb{E}[f(\mathbf{x}^{(R-1)}) - f(\mathbf{x}^{(*)})] \leq \epsilon$ if we set:

205 • **FS-PRIVIX**, for $\eta = \frac{1}{2L(cd/mk+1)\tau\gamma}$:

$$R = O((d/mk + 1) \kappa \log(1/\epsilon)) ,$$

$$\tau = O\left((d/m + 1) / (d/m + k) \epsilon\right) .$$

206 • **FS-HEAPRIX**, for $\eta = \frac{1}{2L((cd-m)/mk+1)\tau\gamma}$:

$$R = O(((d-m)/mk + 1) \kappa \log(1/\epsilon)) ,$$

$$\tau = O\left(d/m / (((d/m - 1) + k) \epsilon)\right) .$$

207 In the **Convex** case, $\{\mathbf{x}^{(r)}\}_{r=0}^R$ satisfies $\mathbb{E}[f(\mathbf{x}^{(R-1)}) - f(\mathbf{x}^{(*)})] \leq \epsilon$ if we set:

208 • **FS-PRIVIX**, for $\eta = \frac{1}{2L(cd/mk+1)\tau\gamma}$:

$$R = O(L(1 + d/mk) / \epsilon \log(1/\epsilon)) ,$$

$$\tau = O\left((d/m + 1)^2 / (k(d/mk + 1)^2 \epsilon^2)\right) .$$

209 • **FS-HEAPRIX**, for $\eta = \frac{1}{2L((cd-m)/mk+1)\tau\gamma}$:

$$R = O(L(1 + (d-m)/mk) / \epsilon \log(1/\epsilon)) ,$$

$$\tau = O\left((d/m)^2 / (k([d-m]/mk + 1)^2 \epsilon^2)\right) .$$

210 The bounds in Theorem 1 suggest that in homogeneous setting if we set $d = m$ (no compression),
 211 the number of communication rounds to achieve the ϵ error matches with the number of iterations
 212 required to achieve the same error under a centralized setting. Additionally, computational complexity
 213 scales down with number of sampled devices. To stress on the further impact of using sketching, we
 214 also compare our results with prior works in terms of total number of communicated bits per device
 215 as follows:

216 **Comparison with Ivkin et al. [17]** From privacy aspect, we note Ivkin et al. [17] requires for
 217 server to have access to exact values of top_m gradients, hence do not preserve privacy, whereas our
 218 schemes do not need those exact values. From communication cost point of view, for strongly convex
 219 objective and compared to Ivkin et al. [17], we improve the total communication per worker from
 220 $RB = O\left(\frac{d}{\epsilon} \log\left(\frac{d}{\delta\sqrt{\epsilon}} \max\left(\frac{d}{m}, \frac{1}{\sqrt{\epsilon}}\right)\right)\right)$ to

$$RB = O\left(\kappa\left(\frac{d-m}{k} + m\right) \log \frac{1}{\epsilon} \log\left(\frac{\kappa d}{\delta}\left(\frac{d-m}{mk} + 1\right) \log \frac{1}{\epsilon}\right)\right) .$$

221 We note that while reducing communication cost, our scheme requires $\tau = O(d/m(k(\frac{d}{mk}+1)\epsilon)) > 1$,
 222 which scales down with the number of sampled devices, k . Moreover, unlike Ivkin et al. [17], we do

not use bounded gradient assumption. Therefore, we obtain stronger result with weaker assumptions. Regarding general non-convex objectives, our result improves the total communication cost per worker in Ivkin et al. [17] from $RB = O\left(\max(\frac{1}{\epsilon^2}, \frac{d^2}{k^2\epsilon}) \log(\frac{d}{\delta} \max(\frac{1}{\epsilon^2}, \frac{d^2}{k^2\epsilon}))\right)$ for *only one device* to $RB = O(\frac{m}{\epsilon} \log(\frac{d}{\epsilon\delta}))$. We also highlight that we can obtain similar rates for Algorithm 3 in heterogeneous environment if we make the additional assumption of uniformly bounded gradient.

Note: Such improved communication cost over prior related works is due to joint exploitation of *sketching*, to reduce the dimension of communicated messages, and the use of *local updates*, to reduce the total number of communication rounds leading to a specific convergence error.

4.2 Convergence of FedSKETCHGATE

We start with bounded local variance assumption:

Assumption 3 (Bounded Local Variance). *For all $j \in [p]$, we can sample an independent mini-batch Ξ_j of size $|\xi_j| = b$ and compute an unbiased stochastic gradient $\tilde{\mathbf{g}}_j = \nabla f_j(\mathbf{x}; \Xi_j)$ with $\mathbb{E}_\xi[\tilde{\mathbf{g}}_j] = \nabla f_j(\mathbf{x}) = \mathbf{g}_j$. Moreover, the variance of local stochastic gradients is bounded such that $\mathbb{E}_\Xi[\|\tilde{\mathbf{g}}_j - \mathbf{g}_j\|^2] \leq \sigma^2$.*

Theorem 2. *Suppose Assumptions 1 and 3 hold. Given $0 < m \leq d$, and considering FedSKETCHGATE in Algorithm 4 with sketch size $B = O(m \log(\frac{dR}{\delta}))$ and $\gamma \geq p$ with probability $1 - \delta$ we have*

*In the **non-convex** case, $\eta = \frac{1}{L\gamma} \sqrt{\frac{mp}{R\tau(cd)}}$, $\{\mathbf{x}^{(r)}\}_{r=0}^\infty$ satisfies $\frac{1}{R} \sum_{r=0}^{R-1} \|\nabla f(\mathbf{x}^{(r)})\|_2^2 \leq \epsilon$ if:*

• **FS-PRIVIX:**

$$R = O((d+m)/m\epsilon) \quad \text{and} \quad \tau = O(1/(p\epsilon)) .$$

• **FS-HEAPRIX:**

$$R = O(d/m\epsilon) \quad \text{and} \quad \tau = O(1/(p\epsilon)) .$$

*In the **PL or Strongly convex** case, $\{\mathbf{x}^{(r)}\}_{r=0}^\infty$ satisfies $\mathbb{E}[f(\mathbf{x}^{(R-1)}) - f(\mathbf{x}^{(*)})] \leq \epsilon$ if:*

• **FS-PRIVIX**, for $\eta = 1/(2L(\frac{cd}{m} + 1)\tau\gamma)$:

$$R = O\left(\left(\frac{d}{m} + 1\right)\kappa \log(1/\epsilon)\right) \quad \text{and} \quad \tau = O(1/(p\epsilon)) .$$

• **FS-HEAPRIX**, for $\eta = m/(2cLd\tau\gamma)$:

$$R = O\left(\left(\frac{d}{m}\right)\kappa \log(1/\epsilon)\right) \quad \text{and} \quad \tau = O(1/(p\epsilon)) .$$

*In the **convex** case, $\{\mathbf{x}^{(r)}\}_{r=0}^\infty$ satisfies $\mathbb{E}[f(\mathbf{x}^{(R-1)}) - f(\mathbf{x}^{(*)})] \leq \epsilon$ if:*

• **FS-PRIVIX**, for $\eta = 1/(2L(cd/m + 1)\tau\gamma)$:

$$R = O(L(d/m + 1)\epsilon \log(1/\epsilon)) \quad \text{and} \quad \tau = O(1/(p\epsilon^2)) .$$

• **FS-HEAPRIX**, for $\eta = m/(2Lcd\tau\gamma)$:

$$R = O(L(d/m)\epsilon \log(1/\epsilon)) \quad \text{and} \quad \tau = O(1/(p\epsilon^2)) .$$

Theorem 2 implies that the number of communication rounds and local updates are similar to the corresponding quantities in homogeneous setting except for the non-convex case where the number of communication rounds also depends on the compression rate.

These results are summarized in Table 2-3 of the Appendix.

4.3 Comparison with Prior Methods

Before comparing with prior works, we highlight that privacy is another purpose of using unbiased sketching in addition to communication efficiency. Therefore, our main competing schemes are distributed algorithms based on sketching. Nonetheless, for the sake of showing the effectiveness of

our algorithms, we also compare with prior non-sketching based distributed algorithms ([20; 3; 36; 13]) in Section B of Appendix.

Comparison with Li et al. [26]. Note that our convergence analysis does not rely on the bounded gradient assumption. We also improve both the number of communication rounds R and the size of transmitted bits B per communication round. Additionally, we highlight that, while [26] provides a convergence analysis for convex objectives, our analysis holds for PL (thus strongly convex case), general convex and general non-convex objectives.

Comparison with Rothchild et al. [37]. Due to gradient tracking, our algorithm tackles data heterogeneity issue, while algorithms in Rothchild et al. [37] does not particularly. As a consequence, in FedSKETCHGATE each device has to store an additional state vector compared to Rothchild et al. [37]. Yet, as our method is built upon an unbiased compressor, server does not need to store any additional error correction vector. The convergence results for both of two variants of FetchSGD in Rothchild et al. [37] rely on the uniform bounded gradient assumption which may not be applicable with L -smoothness assumption when data distribution is highly heterogeneous, as in FL, see [21], while our bounds do not assume such boundedness. Besides, Theorem 1 [37] assumes that *Contraction Holds* for the sequence of gradients which may not hold in practice, yet based on this strong assumption, their total communication cost (RB) in order to achieve ϵ error is $RB = O\left(m \max\left(\frac{1}{\epsilon^2}, \frac{d^2 - dm}{m^2 \epsilon}\right) \log\left(\frac{d}{\delta} \max\left(\frac{1}{\epsilon^2}, \frac{d^2 - dm}{m^2 \epsilon}\right)\right)\right)$. For the sake of comparison we let the compression ratio in Rothchild et al. [37] to be $\frac{m}{d}$. In contrast, without any extra assumptions, our results in Theorem 2 for PRIVIX and HEAPRIX are respectively $RB = O\left(\frac{(d+m)}{\epsilon} \log\left(\frac{(\frac{d^2}{m}) + d}{\epsilon \delta}\right)\right)$ and $RB = O\left(\frac{d}{\epsilon} \log\left(\frac{d^2}{\epsilon m \delta}\right)\right)$ which improves the total communication cost of Theorem 1 in Rothchild et al. [37] under regimes such that $\frac{1}{\epsilon} \geq d$ or $d \gg m$. Theorem 2 in Rothchild et al. [37] is based the *Sliding Window Heavy Hitters* assumption, which is similar to the gradient diversity assumption in Li et al. [29]; Haddadpour and Mahdavi [12]. Under that assumption the total communication cost is shown to be $RB = O\left(\frac{m \max(I^{2/3}, 2 - \alpha)}{\epsilon^3 \alpha} \log\left(\frac{d \max(I^{2/3}, 2 - \alpha)}{\epsilon^3 \delta}\right)\right)$ where I is a constant related to the window of gradients. We improve this bound under weaker assumptions in a regime where $\frac{I^{2/3}}{\epsilon^2} \geq d$. We also provide bounds for PL, convex and non-convex objectives contrary to Rothchild et al. [37]. Finally, we note that algorithms in Rothchild et al. [37] are using momentum at server. While we do not use it explicitly, we can modify our algorithms to include momentum easily.

5 Numerical Study

In this section, we provide empirical results on MNIST benchmark dataset to demonstrate the effectiveness of our proposed algorithms. We train LeNet-5 Convolutional Neural Network (CNN) architecture introduced in LeCun et al. [24], with 60 000 parameters. We compare Federated SGD (FedSGD) as the full-precision baseline, along with four sketching methods SketchSGD [17], FetchSGD [37], and two FedSketch variants FS-PRIVIX and FS-HEAPRIX. Note that in Algorithm 3, FS-PRIVIX with global learning rate $\gamma = 1$ is equivalent to the DiffSketch algorithm proposed in Li et al. [29]. Also, SketchSGD is slightly modified to compress the change in local weights (instead of local gradient in every iteration), and FetchSGD is implemented with second round of communication for fairness. (The original proposal does not include second round of communication, which performs worse with small sketch size.) As suggested in [37], the momentum factor of FetchSGD is set to 0.9, and we also follow some recommended implementation tricks to improve its performance, which are detailed in the Appendix. The number of workers is set to 50 and we report the results for 1 and 5 local epochs. A local epoch is finished when all workers go through their local data samples once. The local batch size is 30. In each round, we randomly choose half of the devices to be active. We tune the learning rates (η and γ , if applicable) over log-scale and report the best results, for both *homogeneous* and *heterogeneous* setting. In the former case, each device receives uniformly drawn data samples, and in the latter, it only receives samples from one or two classes among ten.

Homogeneous case. In Figure 1, we provide the training loss and test accuracy with different number of local epochs and sketch size, $(t, k) = (20, 40)$ and $(50, 100)$. Note that, these two choices of sketch size correspond to a $75\times$ and $12\times$ compression ratio, respectively. We conclude

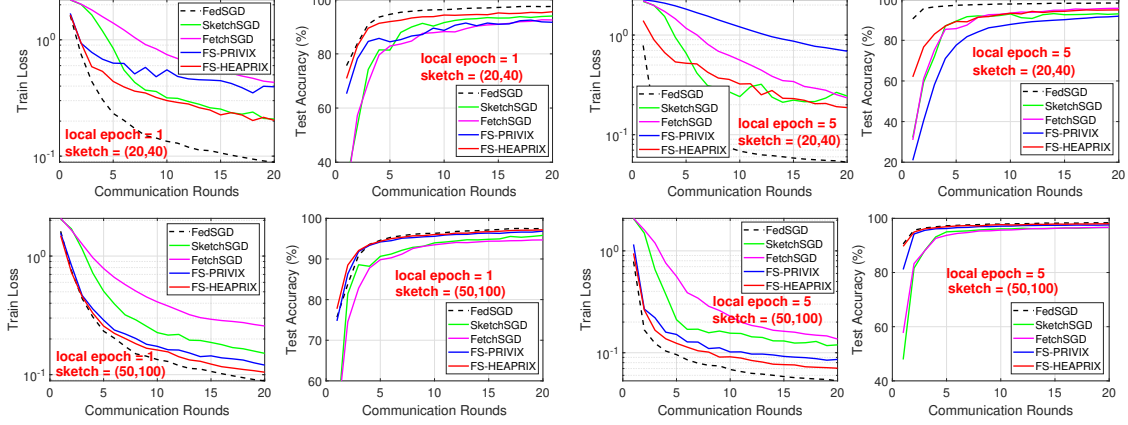


Figure 1: Homogeneous case: Comparison of compressed optimization methods on LeNet CNN.

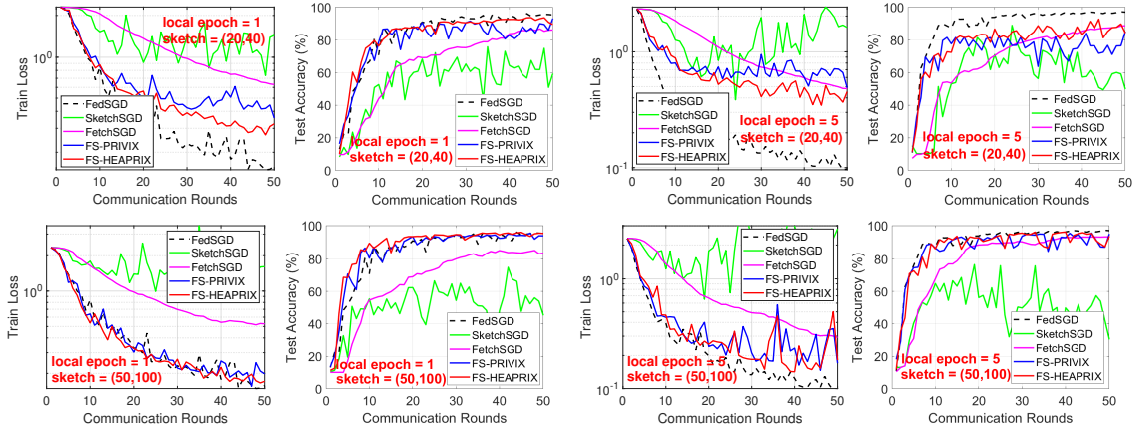


Figure 2: Heterogeneous case: Comparison of compressed optimization algorithms on LeNet CNN.

- In general, increasing compression ratio would sacrifice learning performance. In all cases, FS-HEAPRIX performs the best in terms of both training objective and test accuracy, among all compressed methods.
- FS-HEAPRIX is better than FS-PRIVIX, especially with small sketches (high compression ratio). FS-HEAPRIX yields acceptable extra test error compared to full-precision FedSGD, particularly when considering the high compression ratio (e.g., $75\times$).
- From the training loss, we see that the performance of FS-HEAPRIX improves when the number of local updates increases. *That is, the proposed method is able to further reduce the communication cost by reducing the number of rounds required for communication.* This is also consistent with our theoretical findings.

In general, our proposed FS-HEAPRIX outperforms all competing methods, and a sketch size of (50, 100) is sufficient to approach the accuracy of full-precision FedSGD.

Heterogeneous case. We plot similar set of results in Figure 2 for non-i.i.d. data distribution, which leads to more twists and turns in the training curves. We see that SketchSGD performs very poorly in the heterogeneous case, which is improved by error tracking and momentum in FetchSGD, as expected. However, both of these methods are worse than our proposed FedSketchGATE methods, which can achieve similar generalization accuracy as full-precision FedSGD, even with small sketch size (i.e., $75\times$ compression with 1 local epoch). Note that, slower convergence and worse generalization of FedSGD in non-i.i.d. data distribution case is also reported in e.g. McMahan et al. [33]; Chen et al. [8].

We also notice in Figure 2 the advantage of FS-HEAPRIX over FS-PRIVIX in terms of training loss and test accuracy. However, empirically we see that in the heterogeneous setting, more local

updates tend to undermine the learning performance, especially with small sketch size. Nevertheless, when the sketch size is not too small, i.e., $(50, 100)$, FS-HEAPRIX can still provide comparable test accuracy as FedSGD in both cases. Our empirical study demonstrates that our proposed FedSketch (and FedSketchGATE) frameworks are able to perform well in homogeneous (resp. heterogeneous) setting, with high compression rate. In particular, FedSketch methods are advantageous over recent SketchedSGD [17] and FetchSGD [37] in all cases. FS-HEAPRIX performs the best among all the tested compressed optimization algorithms, which in many cases achieves similar generalization accuracy as full-precision FedSGD with small sketch size.

6 Conclusion

In this paper, we introduced FedSKETCH and FedSKETCHGATE algorithms for homogeneous and heterogeneous data distribution setting respectively for Federated Learning wherein communication between server and devices is only performed using count sketch. Our algorithms, thus, provide communication-efficiency and privacy, through random hashes based sketches. We analyze the convergence error for *non-convex*, *PL* and *general convex* objective functions in the scope of Federated Optimization. We provide insightful numerical experiments showcasing the advantages of our FedSKETCH and FedSKETCHGATE methods over current federated optimization algorithm. The proposed algorithms outperform competing compression method and can achieve comparable test accuracy as Federated SGD, with high compression ratio.

References

- [1] Dan Alistarh, Demjan Grubic, Jerry Li, Ryota Tomioka, and Milan Vojnovic. Qsgd: Communication-efficient sgd via gradient quantization and encoding. In *Advances in Neural Information Processing Systems (NIPS)*, pages 1709–1720, Long Beach, 2017.
- [2] Dan Alistarh, Torsten Hoefler, Mikael Johansson, Nikola Konstantinov, Sarit Khirirat, and Cédric Renggli. The convergence of sparsified gradient methods. In *Advances in Neural Information Processing Systems (NeurIPS)*, pages 5973–5983, Montréal, Canada, 2018.
- [3] Debraj Basu, Deepesh Data, Can Karakus, and Suhas N. Diggavi. Qsparse-local-sgd: Distributed SGD with quantization, sparsification and local computations. In *Advances in Neural Information Processing Systems (NeurIPS)*, pages 14668–14679, Vancouver, Canada, 2019.
- [4] Jeremy Bernstein, Yu-Xiang Wang, Kamyar Azizzadenesheli, and Animashree Anandkumar. SIGNSGD: compressed optimisation for non-convex problems. In *Proceedings of the 35th International Conference on Machine Learning (ICML)*, pages 559–568, Stockholmsmässan, Stockholm, Sweden, 2018.
- [5] Keith Bonawitz, Vladimir Ivanov, Ben Kreuter, Antonio Marcedone, H. Brendan McMahan, Sarvar Patel, Daniel Ramage, Aaron Segal, and Karn Seth. Practical secure aggregation for privacy-preserving machine learning. In *Proceedings of the 2017 ACM SIGSAC Conference on Computer and Communications Security (CCS)*, pages 1175–1191, Dallas, TX, 2017.
- [6] Léon Bottou and Olivier Bousquet. The tradeoffs of large scale learning. In *Advances in Neural Information Processing Systems (NIPS)*, pages 161–168, Vancouver, Canada, 2008.
- [7] Moses Charikar, Kevin C. Chen, and Martin Farach-Colton. Finding frequent items in data streams. *Theoretical Computer Science*, 312(1):3–15, 2004. doi: 10.1016/S0304-3975(03)00400-6. URL [https://doi.org/10.1016/S0304-3975\(03\)00400-6](https://doi.org/10.1016/S0304-3975(03)00400-6).
- [8] Xiangyi Chen, Xiaoyun Li, and Ping Li. Toward communication efficient adaptive gradient method. In *ACM-IMS Foundations of Data Science Conference (FODS)*, Seattle, WA, 2020.
- [9] Graham Cormode and Shan Muthukrishnan. An improved data stream summary: the count-min sketch and its applications. *Journal of Algorithms*, 55(1):58–75, 2005.
- [10] Cynthia Dwork. Differential privacy. In *Automata, Languages and Programming, 33rd International Colloquium, ICALP 2006, Venice, Italy, July 10-14, 2006, Proceedings, Part II*, volume 4052 of *Lecture Notes in Computer Science*, pages 1–12. Springer, 2006.
- [11] Robin C Geyer, Tassilo Klein, and Moin Nabi. Differentially private federated learning: A client level perspective. *arXiv preprint arXiv:1712.07557*, 2017.
- [12] Farzin Haddadpour and Mehrdad Mahdavi. On the convergence of local descent methods in federated learning. *arXiv preprint arXiv:1910.14425*, 2019.
- [13] Farzin Haddadpour, Mohammad Mahdi Kamani, Aryan Mokhtari, and Mehrdad Mahdavi. Federated learning with compression: Unified analysis and sharp guarantees. *arXiv preprint arXiv:2007.01154*, 2020.
- [14] Stephen Hardy, Wilko Henecka, Hamish Ivey-Law, Richard Nock, Giorgio Patrini, Guillaume Smith, and Brian Thorne. Private federated learning on vertically partitioned data via entity resolution and additively homomorphic encryption. *arXiv preprint arXiv:1711.10677*, 2017.
- [15] Samuel Horváth and Peter Richtárik. A better alternative to error feedback for communication-efficient distributed learning. *arXiv preprint arXiv:2006.11077*, 2020.
- [16] Samuel Horváth, Dmitry Kovalev, Konstantin Mishchenko, Sebastian Stich, and Peter Richtárik. Stochastic distributed learning with gradient quantization and variance reduction. *arXiv preprint arXiv:1904.05115*, 2019.

- [17] Nikita Ivkin, Daniel Rothchild, Enayat Ullah, Vladimir Braverman, Ion Stoica, and Raman Arora. Communication-efficient distributed SGD with sketching. In *Advances in Neural Information Processing Systems (NeurIPS)*, pages 13144–13154, Vancouver, Canada, 2019.
- [18] Peter Kairouz, H Brendan McMahan, Brendan Avent, Aurélien Bellet, Mehdi Bennis, Arjun Nitin Bhagoji, Keith Bonawitz, Zachary Charles, Graham Cormode, Rachel Cummings, et al. Advances and open problems in federated learning. *arXiv preprint arXiv:1912.04977*, 2019.
- [19] Hamed Karimi, Julie Nutini, and Mark Schmidt. Linear convergence of gradient and proximal-gradient methods under the polyak-łojasiewicz condition. In *Proceedings of European Conference on Machine Learning and Knowledge Discovery in Databases (ECML-PKDD)*, pages 795–811, Riva del Garda, Italy, 2016.
- [20] Sai Praneeth Karimireddy, Satyen Kale, Mehryar Mohri, Sashank J Reddi, Sebastian U Stich, and Ananda Theertha Suresh. Scaffold: Stochastic controlled averaging for on-device federated learning. *arXiv preprint arXiv:1910.06378*, 2019.
- [21] Ahmed Khaled, Konstantin Mishchenko, and Peter Richtárik. Tighter theory for local SGD on identical and heterogeneous data. In *The 23rd International Conference on Artificial Intelligence and Statistics (AISTATS)*, pages 4519–4529, Online [Palermo, Sicily, Italy], 2020.
- [22] Jon Kleinberg. Bursty and hierarchical structure in streams. *Data Mining and Knowledge Discovery*, 7(4):373–397, 2003.
- [23] Jakub Konečný, H Brendan McMahan, Felix X Yu, Peter Richtárik, Ananda Theertha Suresh, and Dave Bacon. Federated learning: Strategies for improving communication efficiency. *arXiv preprint arXiv:1610.05492*, 2016.
- [24] Yann LeCun, Léon Bottou, Yoshua Bengio, and Patrick Haffner. Gradient-based learning applied to document recognition. *Proceedings of the IEEE*, 86(11):2278–2324, 1998.
- [25] Ping Li, Kenneth Ward Church, and Trevor Hastie. One sketch for all: Theory and application of conditional random sampling. In *Advances in Neural Information Processing Systems (NIPS)*, pages 953–960, Vancouver, Canada, 2008.
- [26] Tian Li, Zaoxing Liu, Vyas Sekar, and Virginia Smith. Privacy for free: Communication-efficient learning with differential privacy using sketches. *arXiv preprint arXiv:1911.00972*, 2019.
- [27] Tian Li, Anit Kumar Sahu, Ameet Talwalkar, and Virginia Smith. Federated learning: Challenges, methods, and future directions. *IEEE Signal Process. Mag.*, 37(3):50–60, 2020.
- [28] Tian Li, Anit Kumar Sahu, Ameet Talwalkar, and Virginia Smith. Federated learning: Challenges, methods, and future directions. *IEEE Signal Processing Magazine*, 37(3):50–60, 2020.
- [29] Tian Li, Anit Kumar Sahu, Manzil Zaheer, Maziar Sanjabi, Ameet Talwalkar, and Virginia Smith. Federated optimization in heterogeneous networks. In *Proceedings of Machine Learning and Systems (MLSys)*, Austin, TX, 2020.
- [30] Xiang Li, Kaixuan Huang, Wenhao Yang, Shusen Wang, and Zhihua Zhang. On the convergence of fedavg on non-iid data. In *Proceedings of the 8th International Conference on Learning Representations (ICLR)*, Addis Ababa, Ethiopia, 2020.
- [31] Xianfeng Liang, Shuheng Shen, Jingchang Liu, Zhen Pan, Enhong Chen, and Yifei Cheng. Variance reduced local sgd with lower communication complexity. *arXiv preprint arXiv:1912.12844*, 2019.
- [32] Yujun Lin, Song Han, Huizi Mao, Yu Wang, and Bill Dally. Deep gradient compression: Reducing the communication bandwidth for distributed training. In *Proceedings of the 6th International Conference on Learning Representations (ICLR)*, Vancouver, Canada, 2018.

- [33] Brendan McMahan, Eider Moore, Daniel Ramage, Seth Hampson, and Blaise Agüera y Arcas. Communication-efficient learning of deep networks from decentralized data. In *Proceedings of the 20th International Conference on Artificial Intelligence and Statistics (AISTATS)*, pages 1273–1282, Fort Lauderdale, FL, 2017.
- [34] H. Brendan McMahan, Daniel Ramage, Kunal Talwar, and Li Zhang. Learning differentially private recurrent language models. In *Proceedings of the 6th International Conference on Learning Representations (ICLR)*, Vancouver, Canada, 2018.
- [35] Constantin Philippenko and Aymeric Dieuleveut. Artemis: tight convergence guarantees for bidirectional compression in federated learning. *arXiv preprint arXiv:2006.14591*, 2020.
- [36] Amirhossein Reisizadeh, Aryan Mokhtari, Hamed Hassani, Ali Jadbabaie, and Ramtin Pedarsani. Fedpaq: A communication-efficient federated learning method with periodic averaging and quantization. In *The 23rd International Conference on Artificial Intelligence and Statistics (AISTATS)*, pages 2021–2031, Online [Palermo, Sicily, Italy], 2020.
- [37] Daniel Rothchild, Ashwinee Panda, Enayat Ullah, Nikita Ivkin, Ion Stoica, Vladimir Braverman, Joseph Gonzalez, and Raman Arora. FetchSGD: Communication-efficient federated learning with sketching. *arXiv preprint arXiv:2007.07682*, 2020.
- [38] Anit Kumar Sahu, Tian Li, Maziar Sanjabi, Manzil Zaheer, Ameet Talwalkar, and Virginia Smith. On the convergence of federated optimization in heterogeneous networks. *arXiv preprint arXiv:1812.06127*, 2018.
- [39] Sebastian U Stich and Sai Praneeth Karimireddy. The error-feedback framework: Better rates for sgd with delayed gradients and compressed communication. *arXiv preprint arXiv:1909.05350*, 2019.
- [40] Sebastian U Stich, Jean-Baptiste Cordonnier, and Martin Jaggi. Sparsified sgd with memory. In *Advances in Neural Information Processing Systems (NeurIPS)*, pages 4447–4458, Montréal, Canada, 2018.
- [41] Sebastian Urban Stich. Local sgd converges fast and communicates little. In *Proceedings of the 7th International Conference on Learning Representations (ICLR)*, New Orleans, LA, 2019.
- [42] Hanlin Tang, Shaoduo Gan, Ce Zhang, Tong Zhang, and Ji Liu. Communication compression for decentralized training. In *Advances in Neural Information Processing Systems (NeurIPS)*, pages 7652–7662, Montréal, Canada, 2018.
- [43] Jianyu Wang and Gauri Joshi. Cooperative sgd: A unified framework for the design and analysis of communication-efficient sgd algorithms. *arXiv preprint arXiv:1808.07576*, 2018.
- [44] Wei Wen, Cong Xu, Feng Yan, Chunpeng Wu, Yandan Wang, Yiran Chen, and Hai Li. Terngrad: Ternary gradients to reduce communication in distributed deep learning. In *Advances in neural information processing systems (NIPS)*, pages 1509–1519, Long Beach, CA, 2017.
- [45] Jiayang Wu, Weidong Huang, Junzhou Huang, and Tong Zhang. Error compensated quantized sgd and its applications to large-scale distributed optimization. *arXiv preprint arXiv:1806.08054*, 2018.
- [46] Hao Yu, Rong Jin, and Sen Yang. On the linear speedup analysis of communication efficient momentum SGD for distributed non-convex optimization. In *Proceedings of the 36th International Conference on Machine Learning (ICML)*, pages 7184–7193, Long Beach, CA, 2019.
- [47] Hao Yu, Sen Yang, and Shenghuo Zhu. Parallel restarted SGD with faster convergence and less communication: Demystifying why model averaging works for deep learning. In *The Thirty-Third AAAI Conference on Artificial Intelligence (AAAI)*, pages 5693–5700, Honolulu, HI, 2019.
- [48] Fan Zhou and Guojing Cong. On the convergence properties of a k-step averaging stochastic gradient descent algorithm for nonconvex optimization. In *Proceedings of the Twenty-Seventh International Joint Conference on Artificial Intelligence (IJCAI)*, pages 3219–3227, Stockholm, Sweden, 2018.

487 A Notations and Definitions

488 **Notation.** Here we denote the count sketch of the vector \mathbf{x} by $\mathbf{S}(\mathbf{x})$ and with an abuse of notation,
 489 we indicate the expectation over the randomness of count sketch with $\mathbb{E}_{\mathbf{S}}[\cdot]$. We illustrate the random
 490 subset of the devices selected by the central server with \mathcal{K} with size $|\mathcal{K}| = k \leq p$, and we represent
 491 the expectation over the device sampling with $\mathbb{E}_{\mathcal{K}}[\cdot]$.

Table 1: Table of Notations

p	\triangleq	Number of devices
k	\triangleq	Number of sampled devices for homogeneous setting
$\mathcal{K}^{(r)}$	\triangleq	Set of sampled devices in communication round r
d	\triangleq	Dimension of the model
τ	\triangleq	Number of local updates
R	\triangleq	Number of communication rounds
B	\triangleq	Size of transmitted bits
$R \times B$	\triangleq	Total communication cost per device
κ	\triangleq	Condition number
ϵ	\triangleq	Target accuracy
μ	\triangleq	PL constant
m	\triangleq	Number of bins of hash tables
$\mathbf{S}(\mathbf{x})$	\triangleq	Count sketch of the vector \mathbf{x}
$\mathbb{U}(\Delta)$	\triangleq	Class of unbiased compressor, see Definition 1

492 **Definition 3** (Polyak-Łojasiewicz). *A function $f(\mathbf{x})$ satisfies the Polyak-Łojasiewicz(PL) condition*
 493 *with constant μ if $\frac{1}{2}\|\nabla f(\mathbf{x})\|_2^2 \geq \mu(f(\mathbf{x}) - f(\mathbf{x}^*))$, $\forall \mathbf{x} \in \mathbb{R}^d$ with \mathbf{x}^* is an optimal solution.*

494 A.1 Count sketch

495 In this paper, we exploit the commonly used Count Sketch [7] which is described in Algorithm 5.

Algorithm 5 Count Sketch (CS) [7]

```

1: Inputs:  $\mathbf{x} \in \mathbb{R}^d, t, k, \mathbf{S}_{m \times t}, h_j(1 \leq i \leq t), \text{sign}_j(1 \leq i \leq t)$ 
2: Compress vector  $\mathbf{x} \in \mathbb{R}^d$  into  $\mathbf{S}(\mathbf{x})$ :
3: for  $x_i \in \mathbf{x}$  do
4:   for  $j = 1, \dots, t$  do
5:      $\mathbf{S}[j][h_j(i)] = \mathbf{S}[j-1][h_{j-1}(i)] + \text{sign}_j(i) \cdot x_i$ 
6:   end for
7: end for
8: return  $\mathbf{S}_{m \times t}(\mathbf{x})$ 

```

496 A.2 PRIVIX and compression error of HEAPRIX

497 For the sake of completeness we review PRIVIX algorithm that is also mentioned in Li et al. [26] as
 498 follows:

Algorithm 6 PRIVIX [26]: Unbiased compressor based on sketching.

```

1: Inputs:  $\mathbf{x} \in \mathbb{R}^d, t, m, \mathbf{S}_{m \times t}, h_j(1 \leq i \leq t), \text{sign}_j(1 \leq i \leq t)$ 
2: Query  $\tilde{\mathbf{x}} \in \mathbb{R}^d$  from  $\mathbf{S}(\mathbf{x})$ :
3: for  $i = 1, \dots, d$  do
4:    $\tilde{x}[i] = \text{Median}\{\text{sign}_j(i) \cdot \mathbf{S}[j][h_j(i)] : 1 \leq j \leq t\}$ 
5: end for
6: Output:  $\tilde{\mathbf{x}}$ 

```

Table 3: Comparison of results with compression and periodic averaging in the heterogeneous setting. UG and PP stand for Unbounded Gradient and Privacy Property respectively.

Reference	non-convex	General Convex	UG	PP
Basu et al. [3] (with $\gamma = m/d$)	$R = O\left(\frac{d}{m\epsilon^{1.5}}\right)$ $\tau = O\left(\frac{m}{p d \sqrt{\epsilon}}\right)$ $B = O(d)$ $RB = O\left(\frac{d^2}{m\epsilon^{1.5}}\right)$	—	✗	✗
Li et al. [26]	—	$R = O\left(\frac{d}{m\epsilon^2}\right)$ $\tau = 1$ $B = O\left(m \log\left(\frac{d^2}{m\epsilon^2\delta}\right)\right)$	✗	✓
Rothchild et al. [37]	$R = O\left(\max\left(\frac{1}{\epsilon^2}, \frac{d^2 - md}{m^2\epsilon}\right)\right)$ $\tau = 1$ $B = O\left(m \log\left(\frac{d}{\delta} \max\left(\frac{1}{\epsilon^2}, \frac{d^2 - md}{m^2\epsilon}\right)\right)\right)$ $RB = O\left(m \max\left(\frac{1}{\epsilon^2}, \frac{d^2 - md}{m^2\epsilon}\right) \log\left(\frac{d}{\delta} \max\left(\frac{1}{\epsilon^2}, \frac{d^2 - md}{m^2\epsilon}\right)\right)\right)$	—	✗	✗
Rothchild et al. [37]	$R = O\left(\frac{\max(I^{2/3}, 2 - \alpha)}{\epsilon^3}\right)$ $\tau = 1$ $B = O\left(\frac{m}{\alpha} \log\left(\frac{d \max(I^{2/3}, 2 - \alpha)}{\epsilon^3\delta}\right)\right)$ $RB = O\left(\frac{m \max(I^{2/3}, 2 - \alpha)}{\epsilon^3\alpha} \log\left(\frac{d \max(I^{2/3}, 2 - \alpha)}{\epsilon^3\delta}\right)\right)$	—	✗	✗
Theorem 2	$R = O\left(\frac{d}{m\epsilon}\right)$ $\tau = O\left(\frac{1}{p\epsilon}\right)$ $B = O\left(m \log\left(\frac{d^2}{m\epsilon\delta}\right)\right)$ $RB = O\left(\frac{d}{\epsilon} \log\left(\frac{d^2}{m\epsilon\delta} \log\left(\frac{1}{\epsilon}\right)\right)\right)$	$R = O\left(\frac{d}{m\epsilon} \log\left(\frac{1}{\epsilon}\right)\right)$ $\tau = O\left(\frac{1}{p\epsilon^2}\right)$ $B = O\left(m \log\left(\frac{d^2}{m\epsilon\delta}\right)\right)$	✓	✓

Regarding the compression error of sketching we restate the following Corollary from the main body of this paper:

Corollary 2. *Based on Theorem 3 of [15] and using Algorithm 2, we have $C(x) \in \mathbb{U}(c\frac{d}{m})$. This shows that unlike PRIVIX (Algorithm 6) the compression noise can be made as small as possible using large size of hash table.*

Proof. The proof simply follows from Theorem 3 in Horváth and Richtárik [15] and Algorithm 2 by setting $\Delta_1 = c\frac{d}{m}$ and $\Delta_2 = 1 + c\frac{d}{m}$ we obtain $\Delta = \Delta_2 + \frac{1 - \Delta_2}{\Delta_1} = c\frac{d}{m} = O\left(\frac{d}{m}\right)$ for the compression error of HEAPRIX. \square

B Summary of comparison of our results with prior works

For the purpose of further clarification, we summarize the comparison of our results with related works. We recall that p is the number of devices, d is the dimension of the model, κ is the condition number, ϵ is the target accuracy, R is the number of communication rounds, and τ is the number of local updates. We start with the homogeneous setting comparison. Comparison of our results and existing ones for homogeneous and heterogeneous setting are given respectively Table 2 and Table 3.

Table 2: Comparison of results with compression and periodic averaging in the homogeneous setting. UG and PP stand for Unbounded Gradient and Privacy Property respectively.

Reference	PL/Strongly Convex	UG	PP
Ivkin et al. [17]	$R = O\left(\max\left(\frac{d}{m\sqrt{\epsilon}}, \frac{1}{\epsilon}\right)\right), \tau = 1, B = O\left(m \log\left(\frac{dR}{\delta}\right)\right)$ $pRB = O\left(\frac{pd}{m\epsilon} \log\left(\frac{d}{\delta\sqrt{\epsilon}} \max\left(\frac{d}{m}, \frac{1}{\sqrt{\epsilon}}\right)\right)\right)$	✗	✗
Theorem 1	$R = O\left(\kappa\left(\frac{d-m}{mk} + 1\right) \log\left(\frac{1}{\epsilon}\right)\right), \tau = O\left(\frac{d}{k\left(\frac{d}{k} + m\right)\epsilon}\right), B = O\left(m \log\left(\frac{dR}{\delta}\right)\right)$ $kRB = O\left(m\kappa(d - m + mk) \log\frac{1}{\epsilon} \log\left(\frac{\kappa(d\frac{d-m}{mk} + d) \log\frac{1}{\epsilon}}{\delta}\right)\right)$	✓	✓

Comparison with Haddadpour et al. [13] and Reisizadeh et al. [36] Convergence analysis of algorithms in [13] relies on unbiased compression, while in this paper our FL algorithm based on HEAPRIX enjoys from unbiased compression with equivalent biased compression variance. Moreover, we highlight that the convergence analysis of FedCOMGATE is based on the extra assumption of boundedness of the difference between the average of compressed vectors and compressed averages of vectors. However, we do not need this extra assumption as it is satisfied naturally due to linearity of sketching. Finally, as pointed out in Remark 2, our algorithms enjoy from a bidirectional compression property, unlike FedCOMGATE in general. Furthermore, since results in [13] improve the communication complexity of FedPAQ algorithm, developed in [36], hence FedSKETCH and FedSKETCHGATE improves the communication complexity obtained in [36].

Comparison with Basu et al. [3]. We note that the algorithm in [3] uses a composed compression and quantization while our algorithm is solely based on compression. So, in order to compare with algorithms in [3] we only consider Qsparse-local-SGD with compression and we let compression factor $\gamma = \frac{m}{d}$ (to compare with the same compression ratio induced with sketch size of mt). For strongly convex objective in Qsparse-local-SGD to achieve convergence error of ϵ they require $R = O\left(\kappa \frac{d}{m\sqrt{\epsilon}}\right)$ and $\tau = O\left(\frac{m}{pd\sqrt{\epsilon}}\right)$, which is improved to $R = O\left(\frac{\kappa d}{m} \log(1/\epsilon)\right)$ and $\tau = O\left(\frac{1}{p\epsilon}\right)$ for PL objectives. Similarly, for non-convex objective [3] requires $R = O\left(\frac{d}{m\epsilon^{1.5}}\right)$ and $\tau = O\left(\frac{m}{pd\sqrt{\epsilon}}\right)$, which is improved to $R = O\left(\frac{d}{m\epsilon}\right)$ and $\tau = O\left(\frac{1}{p\epsilon}\right)$. We note that we reduce communication rounds at the cost of increasing number of local updates (which scales down with number of devices, p). Additionally, we highlight that our FedSKETCHGATE exploits the gradient tracking idea to deal with data heterogeneity, while algorithms in [3] does not develop such mechanism and may suffer from poor convergence in heterogeneous setting. We also note that setting $\tau = 1$ and using top_m compressor, the QSPARSE-local-SGD algorithm becomes similar to distributed SGD with sketching as they both use the error feedback framework to improve the compression variance. Finally, since the average of sparse vectors may not be sparse in general the number of transmitted bits from server to devices in QSPARSE-Local-SGD in [3] may not be sparse in general ($B = O(d)$), however our algorithms enjoy from bidirectional compression properly due to lower dimension and linearity properties of sketching ($B = O(m \log(\frac{Rd}{\delta}))$). Therefore, the total number of bits per device for strongly convex and non-convex objective is improved respectively from $RB = O\left(\kappa \frac{d^2}{m\sqrt{\epsilon}}\right)$ and $RB = O\left(\frac{d^2}{m\epsilon^{1.5}}\right)$ in [3] to $RB = O\left(\kappa d \log(\frac{\kappa d^2}{m\delta} \log(\frac{1}{\epsilon})) \log(1/\epsilon)\right) = O\left(\kappa d \max\left(\log(\frac{\kappa d^2}{m\delta}), \log^2(1/\epsilon)\right)\right)$ and $RB = O\left(\log(\frac{d^2}{m\epsilon\delta}) \frac{d}{\epsilon}\right)$.

Additionally, as we noted using sketching for transmission implies two way communication from master to devices and vice versa. Therefore, in order to show efficacy of our algorithm we compare our convergence analysis with the obtained rates in the following related work:

Comparison with Philippenko and Dieuleveut [35]. The reference [35] considers two-way compression from parameter server to devices and vice versa. They provide the convergence rate of $R = O\left(\frac{\omega^{\text{Up}} \omega^{\text{Down}}}{\epsilon^2}\right)$ for strongly-objective functions where ω^{Up} and ω^{Down} are uplink and downlink's compression noise (specializing to our case for the sake of comparison $\omega^{\text{Up}} = \omega^{\text{Down}} = \theta(d)$) for general heterogeneous data distribution. In contrast, while our algorithms are using bidirectional compression due to use of sketching for communication, our convergence rate for strongly-convex objective is $R = O(\kappa \mu^2 d \log(\frac{1}{\epsilon}))$ with probability $1 - \delta$.

C Theoretical Proofs

We will use the following fact (which is also used in Li et al. [30]; Haddadpour and Mahdavi [12]) in proving results.

Fact 3 (Li et al. [30]; Haddadpour and Mahdavi [12]). *Let $\{x_i\}_{i=1}^p$ denote any fixed deterministic sequence. We sample a multiset \mathcal{P} (with size K) uniformly at random where x_j is sampled with probability q_j for $1 \leq j \leq p$ with replacement. Let $\mathcal{P} = \{i_1, \dots, i_K\} \subset [p]$ (some i_j s may have the*

560 same value). Then

$$\mathbb{E}_{\mathcal{P}} \left[\sum_{i \in \mathcal{P}} x_i \right] = \mathbb{E}_{\mathcal{P}} \left[\sum_{k=1}^K x_{i_k} \right] = K \mathbb{E}_{\mathcal{P}} [x_{i_k}] = K \left[\sum_{j=1}^p q_j x_j \right] \quad (2)$$

561 For the sake of the simplicity, we review an assumption for the quantization/compression, that
 562 naturally holds for PRIVIX and HEAPRIX.

563 **Assumption 4** (Haddadpour et al. [13]). *The output of the compression operator $Q(\mathbf{x})$ is an unbiased*
 564 *estimator of its input \mathbf{x} , and its variance grows with the squared of the squared of ℓ_2 -norm of its*
 565 *argument, i.e., $\mathbb{E}[Q(\mathbf{x})] = \mathbf{x}$ and $\mathbb{E}[\|Q(\mathbf{x}) - \mathbf{x}\|^2] \leq \omega \|\mathbf{x}\|^2$.*

566 We note that the sketching PRIVIX and HEAPRIX, satisfy Assumption 4 with $\omega = c \frac{d}{m}$ and $\omega =$
 567 $c \frac{d}{m} - 1$ respectively with probability $1 - \frac{\delta}{R}$ per communication round. Therefore, all the results in
 568 Theorem 1, by taking union over the all probabilities of each communication rounds, are concluded
 569 with probability $1 - \delta$ by plugging $\omega = c \frac{d}{m}$ and $\omega = c \frac{d}{m} - 1$ respectively into the corresponding
 570 convergence bounds.

571 C.1 Proof of Theorem 1

572 In this section, we study the convergence properties of our FedSKETCH method presented in Algo-
 573 rithm 3. Before developing the proofs for FedSKETCH in the homogeneous setting, we first mention
 574 the following intermediate lemmas.

575 **Lemma 1.** *Using unbiased compression and under Assumption 2, we have the following bound:*

$$\mathbb{E}_{\mathcal{K}} \left[\mathbb{E}_{\mathbf{S}, \xi^{(r)}} \left[\|\tilde{\mathbf{g}}_{\mathbf{S}}^{(r)}\|^2 \right] \right] = \mathbb{E}_{\xi^{(r)}} \mathbb{E}_{\mathbf{S}} \left[\|\tilde{\mathbf{g}}_{\mathbf{S}}^{(r)}\|^2 \right] \leq \tau \left(\frac{\omega}{k} + 1 \right) \sum_{j=1}^m q_j \left[\sum_{c=0}^{\tau-1} \|\mathbf{g}_j^{(c,r)}\|^2 + \sigma^2 \right] \quad (3)$$

Proof.

$$\begin{aligned} & \mathbb{E}_{\xi^{(r)} | \mathbf{w}^{(r)}} \mathbb{E}_{\mathcal{K}} \left[\mathbb{E}_{\mathbf{S}} \left[\left\| \frac{1}{k} \sum_{j \in \mathcal{K}} \mathbf{S} \left(\sum_{c=0}^{\tau-1} \tilde{\mathbf{g}}_j^{(c,r)} \right) \right\|^2 \right] \right] \\ &= \mathbb{E}_{\xi^{(r)}} \left[\mathbb{E}_{\mathcal{K}} \left[\mathbb{E}_{\mathbf{S}} \left[\left\| \frac{1}{k} \sum_{j \in \mathcal{K}} \mathbf{S} \left(\underbrace{\sum_{c=0}^{\tau-1} \tilde{\mathbf{g}}_j^{(c,r)}}_{\tilde{\mathbf{g}}_{\mathbf{S}_j}^{(r)}} \right) \right\|^2 \right] \right] \right] \\ &\stackrel{\textcircled{1}}{=} \mathbb{E}_{\xi^{(r)}} \left[\mathbb{E}_{\mathcal{K}} \left[\left\| \frac{1}{k} \sum_{j \in \mathcal{K}} \tilde{\mathbf{g}}_{\mathbf{S}_j}^{(r)} - \frac{1}{k} \sum_{j \in \mathcal{K}} \mathbb{E}_{\mathbf{S}} \left[\tilde{\mathbf{g}}_{\mathbf{S}_j}^{(r)} \right] \right\|^2 + \left\| \mathbb{E}_{\mathbf{S}} \left[\frac{1}{k} \sum_{j \in \mathcal{K}} \tilde{\mathbf{g}}_{\mathbf{S}_j}^{(r)} \right] \right\|^2 \right] \right] \\ &\stackrel{\textcircled{2}}{=} \mathbb{E}_{\xi^{(r)}} \left[\mathbb{E}_{\mathcal{K}} \left[\mathbb{E}_{\mathbf{S}} \left[\left\| \frac{1}{k} \left[\sum_{j \in \mathcal{K}} \tilde{\mathbf{g}}_{\mathbf{S}_j}^{(r)} - \sum_{j \in \mathcal{K}} \tilde{\mathbf{g}}_j^{(r)} \right] \right\|^2 + \left\| \frac{1}{k} \sum_{j \in \mathcal{K}} \tilde{\mathbf{g}}_j^{(r)} \right\|^2 \right] \right] \right] \\ &= \mathbb{E}_{\xi^{(r)}} \left[\mathbb{E}_{\mathcal{K}} \left[\left[\text{Var}_{\mathbf{S}} \left[\frac{1}{k} \sum_{j \in \mathcal{K}} \tilde{\mathbf{g}}_{\mathbf{S}_j}^{(r)} \right] \right] + \left\| \frac{1}{k} \sum_{j \in \mathcal{K}} \tilde{\mathbf{g}}_j^{(r)} \right\|^2 \right] \right] \\ &= \mathbb{E}_{\xi^{(r)}} \left[\mathbb{E}_{\mathcal{K}} \left[\left[\frac{1}{k^2} \sum_{j \in \mathcal{K}} \text{Var}_{\mathbf{S}_j} \left[\tilde{\mathbf{g}}_{\mathbf{S}_j}^{(r)} \right] + \left\| \frac{1}{k} \sum_{j \in \mathcal{K}} \tilde{\mathbf{g}}_j^{(r)} \right\|^2 \right] \right] \right] \end{aligned}$$

$$\begin{aligned}
&\leq \mathbb{E}_{\xi^{(r)}} \left[\mathbb{E}_{\mathcal{K}} \left[\frac{1}{k^2} \sum_{j \in \mathcal{K}} \omega \left\| \tilde{\mathbf{g}}_j^{(r)} \right\|^2 + \left\| \frac{1}{k} \sum_{j \in \mathcal{K}} \tilde{\mathbf{g}}_j^{(r)} \right\|^2 \right] \right] \\
&= \left[\mathbb{E}_{\xi} \left[\frac{1}{k} \sum_{j \in \mathcal{K}} \omega \left\| \tilde{\mathbf{g}}_j^{(r)} \right\|^2 + \mathbb{E}_{\mathcal{K}} \mathbb{E}_{\xi^{(r)}} \left\| \frac{1}{k} \sum_{j \in \mathcal{K}} \tilde{\mathbf{g}}_j^{(r)} \right\|^2 \right] \right] \\
&= \left[\mathbb{E}_{\xi} \left[\frac{\omega}{k} \sum_{j=1}^p q_j \left\| \tilde{\mathbf{g}}_j^{(r)} \right\|^2 + \mathbb{E}_{\mathcal{K}} \left[\text{Var} \left(\frac{1}{k} \sum_{j \in \mathcal{K}} \tilde{\mathbf{g}}_j^{(r)} \right) + \left\| \frac{1}{k} \sum_{j \in \mathcal{K}} \mathbf{g}_j^{(r)} \right\|^2 \right] \right] \right] \\
&= \frac{\omega}{k} \sum_{j=1}^p q_j \mathbb{E}_{\xi} \left\| \tilde{\mathbf{g}}_j^{(r)} \right\|^2 + \mathbb{E}_{\mathcal{K}} \left[\frac{1}{k^2} \sum_{j \in \mathcal{K}} \text{Var} \left(\tilde{\mathbf{g}}_j^{(r)} \right) + \left\| \frac{1}{k} \sum_{j \in \mathcal{K}} \mathbf{g}_j^{(r)} \right\|^2 \right] \\
&\leq \frac{\omega}{k} \sum_{j=1}^p q_j \mathbb{E}_{\xi} \left\| \tilde{\mathbf{g}}_j^{(r)} \right\|^2 + \mathbb{E}_{\mathcal{K}} \left[\frac{1}{k^2} \sum_{j \in \mathcal{K}} \tau \sigma^2 + \frac{1}{k} \sum_{j \in \mathcal{K}} \left\| \mathbf{g}_j^{(r)} \right\|^2 \right] \\
&= \frac{\omega}{k} \sum_{j=1}^p q_j \left[\text{Var} \left(\tilde{\mathbf{g}}_j^{(r)} \right) + \left\| \mathbf{g}_j^{(r)} \right\|^2 \right] + \left[\frac{\tau \sigma^2}{k} + \sum_{j=1}^p q_j \left\| \mathbf{g}_j^{(r)} \right\|^2 \right] \\
&\leq \frac{\omega}{k} \sum_{j=1}^p q_j \left[\tau \sigma^2 + \left\| \mathbf{g}_j^{(r)} \right\|^2 \right] + \left[\frac{\tau \sigma^2}{k} + \sum_{j=1}^p q_j \left\| \mathbf{g}_j^{(r)} \right\|^2 \right] \\
&= (\omega + 1) \frac{\tau \sigma^2}{k} + \left(\frac{\omega}{k} + 1 \right) \left[\sum_{j=1}^p q_j \left\| \mathbf{g}_j^{(r)} \right\|^2 \right] \tag{4}
\end{aligned}$$

576 where ① holds due to $\mathbb{E} \left[\left\| \mathbf{x} \right\|^2 \right] = \text{Var}[\mathbf{x}] + \left\| \mathbb{E}[\mathbf{x}] \right\|^2$, ② is due to $\mathbb{E}_{\mathbf{S}} \left[\frac{1}{p} \sum_{j=1}^p \tilde{\mathbf{g}}_{\mathbf{S}j}^{(r)} \right] = \frac{1}{p} \sum_{j=1}^m \tilde{\mathbf{g}}_j^{(r)}$.

577 Next we show that from Assumptions 3, we have

$$578 \quad \mathbb{E}_{\xi^{(r)}} \left[\left\| \tilde{\mathbf{g}}_j^{(r)} - \mathbf{g}_j^{(r)} \right\|^2 \right] \leq \tau \sigma^2 \tag{5}$$

To do so, note that

$$\begin{aligned}
\text{Var} \left(\tilde{\mathbf{g}}_j^{(r)} \right) &= \mathbb{E}_{\xi^{(r)}} \left[\left\| \tilde{\mathbf{g}}_j^{(r)} - \mathbf{g}_j^{(r)} \right\|^2 \right] \stackrel{\text{①}}{=} \mathbb{E}_{\xi^{(r)}} \left[\left\| \sum_{c=0}^{\tau-1} \left[\tilde{\mathbf{g}}_j^{(c,r)} - \mathbf{g}_j^{(c,r)} \right] \right\|^2 \right] = \text{Var} \left(\sum_{c=0}^{\tau-1} \tilde{\mathbf{g}}_j^{(c,r)} \right) \\
&\stackrel{\text{②}}{=} \sum_{c=0}^{\tau-1} \text{Var} \left(\tilde{\mathbf{g}}_j^{(c,r)} \right) \\
&= \sum_{c=0}^{\tau-1} \mathbb{E} \left[\left\| \tilde{\mathbf{g}}_j^{(c,r)} - \mathbf{g}_j^{(c,r)} \right\|^2 \right] \\
&\stackrel{\text{③}}{\leq} \tau \sigma^2 \tag{6}
\end{aligned}$$

579 where in ① we use the definition of $\tilde{\mathbf{g}}_j^{(r)}$ and $\mathbf{g}_j^{(r)}$, in ② we use the fact that mini-batches are chosen
580 in i.i.d. manner at each local machine, and ③ immediately follows from Assumptions 2.

581 Replacing $\mathbb{E}_{\xi^{(r)}} \left[\left\| \tilde{\mathbf{g}}_j^{(r)} - \mathbf{g}_j^{(r)} \right\|^2 \right]$ in (4) by its upper bound in (5) implies that

$$\mathbb{E}_{\xi^{(r)} | \mathbf{w}^{(r)}} \mathbb{E}_{\mathbf{S}, \mathcal{K}} \left[\left\| \frac{1}{k} \sum_{j \in \mathcal{K}} \mathbf{S} \left(\sum_{c=0}^{\tau-1} \tilde{\mathbf{g}}_j^{(c,r)} \right) \right\|^2 \right] \leq (\omega + 1) \frac{\tau \sigma^2}{k} + \left(\frac{\omega}{k} + 1 \right) \sum_{j=1}^p q_j \left\| \mathbf{g}_j^{(r)} \right\|^2 \tag{7}$$

582 Further note that we have

$$\left\| \mathbf{g}_j^{(r)} \right\|^2 = \left\| \sum_{c=0}^{\tau-1} \mathbf{g}_j^{(c,r)} \right\|^2 \leq \tau \sum_{c=0}^{\tau-1} \left\| \mathbf{g}_j^{(c,r)} \right\|^2 \tag{8}$$

583 where the last inequality is due to $\left\|\sum_{j=1}^n \mathbf{a}_i\right\|^2 \leq n \sum_{j=1}^n \|\mathbf{a}_i\|^2$, which together with (7) leads to
 584 the following bound:

$$\mathbb{E}_{\xi^{(r)}|\mathbf{w}^{(r)}} \mathbb{E}_{\mathbf{S}} \left[\left\| \frac{1}{k} \sum_{j \in \mathcal{K}} \mathbf{S} \left(\sum_{c=0}^{\tau-1} \tilde{\mathbf{g}}_j^{(c,r)} \right) \right\|^2 \right] \leq (\omega + 1) \frac{\tau \sigma^2}{k} + \tau \left(\frac{\omega}{k} + 1 \right) \sum_{j=1}^p q_j \|\mathbf{g}_j^{(c,r)}\|^2, \quad (9)$$

585 and the proof is complete. \square

586 **Lemma 2.** Under Assumption 1, and according to the FedCOM algorithm the expected inner product
 587 between stochastic gradient and full batch gradient can be bounded with:

$$-\mathbb{E}_{\xi, \mathbf{S}, \mathcal{K}} \left[\left\langle \nabla f(\mathbf{w}^{(r)}), \tilde{\mathbf{g}}^{(r)} \right\rangle \right] \leq \frac{1}{2} \eta \frac{1}{m} \sum_{j=1}^m \sum_{c=0}^{\tau-1} \left[-\|\nabla f(\mathbf{w}^{(r)})\|_2^2 - \|\nabla f(\mathbf{w}_j^{(c,r)})\|_2^2 + L^2 \|\mathbf{w}^{(r)} - \mathbf{w}_j^{(c,r)}\|_2^2 \right] \quad (10)$$

588 *Proof.* We have:

$$\begin{aligned} & -\mathbb{E}_{\{\xi_1^{(t)}, \dots, \xi_m^{(t)} | \mathbf{w}_1^{(t)}, \dots, \mathbf{w}_m^{(t)}\}} \mathbb{E}_{\mathbf{S}, \mathcal{K}} \left[\left\langle \nabla f(\mathbf{w}^{(r)}), \tilde{\mathbf{g}}_{\mathbf{S}, \mathcal{K}}^{(r)} \right\rangle \right] \\ &= -\mathbb{E}_{\{\xi_1^{(t)}, \dots, \xi_m^{(t)} | \mathbf{w}_1^{(t)}, \dots, \mathbf{w}_m^{(t)}\}} \left[\left\langle \nabla f(\mathbf{w}^{(r)}), \eta \sum_{j \in \mathcal{K}} q_j \sum_{c=0}^{\tau-1} \tilde{\mathbf{g}}_j^{(c,r)} \right\rangle \right] \\ &= -\left\langle \nabla f(\mathbf{w}^{(r)}), \eta \sum_{j=1}^m q_j \sum_{c=0}^{\tau-1} \mathbb{E}_{\xi, \mathbf{S}} \left[\tilde{\mathbf{g}}_{j, \mathbf{S}}^{(c,r)} \right] \right\rangle \\ &= -\eta \sum_{c=0}^{\tau-1} \sum_{j=1}^m q_j \left\langle \nabla f(\mathbf{w}^{(r)}), \mathbf{g}_j^{(c,r)} \right\rangle \\ &\stackrel{\textcircled{1}}{=} \frac{1}{2} \eta \sum_{c=0}^{\tau-1} \sum_{j=1}^m q_j \left[-\|\nabla f(\mathbf{w}^{(r)})\|_2^2 - \|\nabla f(\mathbf{w}_j^{(c,r)})\|_2^2 + \|\nabla f(\mathbf{w}^{(r)}) - \nabla f(\mathbf{w}_j^{(c,r)})\|_2^2 \right] \\ &\stackrel{\textcircled{2}}{\leq} \frac{1}{2} \eta \sum_{c=0}^{\tau-1} \sum_{j=1}^m q_j \left[-\|\nabla f(\mathbf{w}^{(r)})\|_2^2 - \|\nabla f(\mathbf{w}_j^{(c,r)})\|_2^2 + L^2 \|\mathbf{w}^{(r)} - \mathbf{w}_j^{(c,r)}\|_2^2 \right] \end{aligned} \quad (11)$$

589 where ① is due to $2\langle \mathbf{a}, \mathbf{b} \rangle = \|\mathbf{a}\|^2 + \|\mathbf{b}\|^2 - \|\mathbf{a} - \mathbf{b}\|^2$, and ② follows from Assumption 1. \square

590 The following lemma bounds the distance of local solutions from global solution at r th communication
 591 round.

592 **Lemma 3.** Under Assumptions 2 we have:

$$\mathbb{E} \left[\|\mathbf{w}^{(r)} - \mathbf{w}_j^{(c,r)}\|_2^2 \right] \leq \eta^2 \tau \sum_{c=0}^{\tau-1} \left\| \mathbf{g}_j^{(c,r)} \right\|_2^2 + \eta^2 \tau \sigma^2$$

593 *Proof.* Note that

$$\begin{aligned} \mathbb{E} \left[\left\| \mathbf{w}^{(r)} - \mathbf{w}_j^{(c,r)} \right\|_2^2 \right] &= \mathbb{E} \left[\left\| \mathbf{w}^{(r)} - \left(\mathbf{w}^{(r)} - \eta \sum_{k=0}^c \tilde{\mathbf{g}}_j^{(k,r)} \right) \right\|_2^2 \right] \\ &= \mathbb{E} \left[\left\| \eta \sum_{k=0}^c \tilde{\mathbf{g}}_j^{(k,r)} \right\|_2^2 \right] \\ &\stackrel{\textcircled{1}}{=} \mathbb{E} \left[\left\| \eta \sum_{k=0}^c (\tilde{\mathbf{g}}_j^{(k,r)} - \mathbf{g}_j^{(k,r)}) \right\|_2^2 \right] + \mathbb{E} \left[\left\| \eta \sum_{k=0}^c \mathbf{g}_j^{(k,r)} \right\|_2^2 \right] \end{aligned}$$

$$\begin{aligned}
& \stackrel{\textcircled{2}}{=} \eta^2 \sum_{k=0}^c \mathbb{E} \left[\left\| \left(\tilde{\mathbf{g}}_j^{(k,r)} - \mathbf{g}_j^{(k,r)} \right) \right\|_2^2 \right] + (c+1) \eta^2 \sum_{k=0}^c \left[\left\| \mathbf{g}_j^{(k,r)} \right\|_2^2 \right] \\
& \leq \eta^2 \sum_{k=0}^{\tau-1} \mathbb{E} \left[\left\| \left(\tilde{\mathbf{g}}_j^{(k,r)} - \mathbf{g}_j^{(k,r)} \right) \right\|_2^2 \right] + \tau \eta^2 \sum_{k=0}^{\tau-1} \left[\left\| \mathbf{g}_j^{(k,r)} \right\|_2^2 \right] \\
& \stackrel{\textcircled{3}}{\leq} \eta^2 \sum_{k=0}^{\tau-1} \sigma^2 + \tau \eta^2 \sum_{k=0}^{\tau-1} \left[\left\| \mathbf{g}_j^{(k,r)} \right\|_2^2 \right] \\
& = \eta^2 \tau \sigma^2 + \eta^2 \sum_{k=0}^{\tau-1} \tau \left\| \mathbf{g}_j^{(k,r)} \right\|_2^2
\end{aligned} \tag{12}$$

where ① comes from $\mathbb{E}[\mathbf{x}^2] = \text{Var}[\mathbf{x}] + [\mathbb{E}[\mathbf{x}]]^2$ and ② holds because $\text{Var}\left(\sum_{j=1}^n \mathbf{x}_j\right) = \sum_{j=1}^n \text{Var}(\mathbf{x}_j)$ for i.i.d. vectors \mathbf{x}_i (and i.i.d. assumption comes from i.i.d. sampling), and finally ③ follows from Assumption 2. \square

597 C.1.1 Main result for the non-convex setting

598 Now we are ready to present our result for the homogeneous setting. We first state and prove the
599 result for the general non-convex objectives.

600 **Theorem 4** (non-convex). *For FedSKETCH(τ, η, γ), for all $0 \leq t \leq R\tau - 1$, under Assumptions 1
601 to 2, if the learning rate satisfies*

$$1 \geq \tau^2 L^2 \eta^2 + \left(\frac{\omega}{k} + 1 \right) \eta \gamma L \tau \tag{13}$$

602 *and all local model parameters are initialized at the same point $\mathbf{w}^{(0)}$, then the average-squared
603 gradient after τ iterations is bounded as follows:*

$$\frac{1}{R} \sum_{r=0}^{R-1} \left\| \nabla f(\mathbf{w}^{(r)}) \right\|_2^2 \leq \frac{2(f(\mathbf{w}^{(0)}) - f(\mathbf{w}^{(*)}))}{\eta \gamma \tau R} + \frac{L \eta \gamma (\omega + 1)}{k} \sigma^2 + L^2 \eta^2 \tau \sigma^2, \tag{14}$$

604 *where $\mathbf{w}^{(*)}$ is the global optimal solution with function value $f(\mathbf{w}^{(*)})$.*

605 *Proof.* Before proceeding with the proof of Theorem 4, we would like to highlight that

$$\mathbf{w}^{(r)} - \mathbf{w}_j^{(\tau,r)} = \eta \sum_{c=0}^{\tau-1} \tilde{\mathbf{g}}_j^{(c,r)}. \tag{15}$$

606 From the updating rule of Algorithm 3 we have

$$\mathbf{w}^{(r+1)} = \mathbf{w}^{(r)} - \gamma \eta \left(\frac{1}{k} \sum_{j \in \mathcal{K}} \mathbf{S} \left(\sum_{c=0, r}^{\tau-1} \tilde{\mathbf{g}}_j^{(c,r)} \right) \right) = \mathbf{w}^{(r)} - \gamma \left[\frac{\eta}{k} \sum_{j \in \mathcal{K}} \mathbf{S} \left(\sum_{c=0}^{\tau-1} \tilde{\mathbf{g}}_j^{(c,r)} \right) \right].$$

In what follows, we use the following notation to denote the stochastic gradient used to update the global model at r th communication round

$$\tilde{\mathbf{g}}_{\mathbf{S}, \mathcal{K}}^{(r)} \triangleq \frac{\eta}{p} \sum_{j=1}^p \mathbf{S} \left(\frac{\mathbf{w}^{(r)} - \mathbf{w}_j^{(\tau,r)}}{\eta} \right) = \frac{1}{k} \sum_{j \in \mathcal{K}} \mathbf{S} \left(\sum_{c=0}^{\tau-1} \tilde{\mathbf{g}}_j^{(c,r)} \right).$$

607 and notice that $\mathbf{w}^{(r)} = \mathbf{w}^{(r-1)} - \gamma \tilde{\mathbf{g}}^{(r)}$.

608 Then using the unbiased estimation property of sketching we have:

$$\mathbb{E}_{\mathbf{S}} \left[\tilde{\mathbf{g}}_{\mathbf{S}}^{(r)} \right] = \frac{1}{k} \sum_{j \in \mathcal{K}} \left[-\eta \mathbb{E}_{\mathbf{S}} \left[\mathbf{S} \left(\sum_{c=0}^{\tau-1} \tilde{\mathbf{g}}_j^{(c,r)} \right) \right] \right] = \frac{1}{k} \sum_{j \in \mathcal{K}} \left[-\eta \left(\sum_{c=0}^{\tau-1} \tilde{\mathbf{g}}_j^{(c,r)} \right) \right] \triangleq \tilde{\mathbf{g}}_{\mathbf{S}, \mathcal{K}}^{(r)}.$$

609 From the L -smoothness gradient assumption on global objective, by using $\tilde{\mathbf{g}}^{(r)}$ in inequality (15) we
 610 have:

$$f(\mathbf{w}^{(r+1)}) - f(\mathbf{w}^{(r)}) \leq -\gamma \langle \nabla f(\mathbf{w}^{(r)}), \tilde{\mathbf{g}}^{(r)} \rangle + \frac{\gamma^2 L}{2} \|\tilde{\mathbf{g}}^{(r)}\|^2 \quad (16)$$

611 By taking expectation on both sides of above inequality over sampling, we get:

$$\begin{aligned} \mathbb{E} \left[\mathbb{E}_{\mathbf{S}} \left[f(\mathbf{w}^{(r+1)}) - f(\mathbf{w}^{(r)}) \right] \right] &\leq -\gamma \mathbb{E} \left[\mathbb{E}_{\mathbf{S}} \left[\langle \nabla f(\mathbf{w}^{(r)}), \tilde{\mathbf{g}}_{\mathbf{S}}^{(r)} \rangle \right] \right] + \frac{\gamma^2 L}{2} \mathbb{E} \left[\mathbb{E}_{\mathbf{S}} \|\tilde{\mathbf{g}}_{\mathbf{S}}^{(r)}\|^2 \right] \\ &\stackrel{(a)}{=} -\gamma \underbrace{\mathbb{E} \left[\langle \nabla f(\mathbf{w}^{(r)}), \tilde{\mathbf{g}}^{(r)} \rangle \right]}_{(I)} + \frac{\gamma^2 L}{2} \underbrace{\mathbb{E} \left[\mathbb{E}_{\mathbf{S}} \left[\|\tilde{\mathbf{g}}_{\mathbf{S}}^{(r)}\|^2 \right] \right]}_{(II)}. \end{aligned} \quad (17)$$

612 We proceed to use Lemma 1, Lemma 2, and Lemma 3, to bound terms (I) and (II) in right hand side
 613 of (17), which gives

$$\begin{aligned} &\mathbb{E} \left[\mathbb{E}_{\mathbf{S}} \left[f(\mathbf{w}^{(r+1)}) - f(\mathbf{w}^{(r)}) \right] \right] \\ &\leq \gamma \frac{1}{2} \eta \sum_{j=1}^p q_j \sum_{c=0}^{\tau-1} \left[-\left\| \nabla f(\mathbf{w}^{(r)}) \right\|_2^2 - \left\| \mathbf{g}_j^{(c,r)} \right\|_2^2 + L^2 \eta^2 \sum_{c=0}^{\tau-1} \left[\tau \left\| \mathbf{g}_j^{(c,r)} \right\|_2^2 + \sigma^2 \right] \right] \\ &\quad + \frac{\gamma^2 L (\frac{\omega}{k} + 1)}{2} \left[\eta^2 \tau \sum_{j=1}^p q_j \sum_{c=0}^{\tau-1} \left\| \mathbf{g}_j^{(c,r)} \right\|_2^2 \right] + \frac{\gamma^2 \eta^2 L (\omega + 1)}{2} \frac{\tau \sigma^2}{k} \\ &\stackrel{\textcircled{1}}{\leq} \frac{\gamma \eta}{2} \sum_{j=1}^p q_j \sum_{c=0}^{\tau-1} \left[-\left\| \nabla f(\mathbf{w}^{(r)}) \right\|_2^2 - \left\| \mathbf{g}_j^{(c,r)} \right\|_2^2 + \tau L^2 \eta^2 \left[\tau \left\| \mathbf{g}_j^{(c,r)} \right\|_2^2 + \sigma^2 \right] \right] \\ &\quad + \frac{\gamma^2 L (\frac{\omega}{k} + 1)}{2} \left[\eta^2 \tau \sum_{j=1}^p q_j \sum_{c=0}^{\tau-1} \left\| \mathbf{g}_j^{(c,r)} \right\|_2^2 \right] + \frac{\gamma^2 \eta^2 L (\omega + 1)}{2} \frac{\tau \sigma^2}{k} \\ &= -\eta \gamma \frac{\tau}{2} \left\| \nabla f(\mathbf{w}^{(r)}) \right\|_2^2 \\ &\quad - \left(1 - \tau L^2 \eta^2 \tau - \left(\frac{\omega}{k} + 1 \right) \eta \gamma L \tau \right) \frac{\eta \gamma}{2} \sum_{j=1}^p q_j \sum_{c=0}^{\tau-1} \left\| \mathbf{g}_j^{(c,r)} \right\|_2^2 + \frac{L \tau \gamma \eta^2}{2k} (k L \tau \eta + \gamma (\omega + 1)) \sigma^2 \\ &\stackrel{\textcircled{2}}{\leq} -\eta \gamma \frac{\tau}{2} \left\| \nabla f(\mathbf{w}^{(r)}) \right\|_2^2 + \frac{L \tau \gamma \eta^2}{2k} (k L \tau \eta + \gamma (\omega + 1)) \sigma^2, \end{aligned} \quad (18)$$

614 where in ① we incorporate outer summation $\sum_{c=0}^{\tau-1}$, and ② follows from condition

$$1 \geq \tau L^2 \eta^2 \tau + \left(\frac{\omega}{k} + 1 \right) \eta \gamma L \tau.$$

615 Summing up for all R communication rounds and rearranging the terms gives:

$$\frac{1}{R} \sum_{r=0}^{R-1} \left\| \nabla f(\mathbf{w}^{(r)}) \right\|_2^2 \leq \frac{2 (f(\mathbf{w}^{(0)}) - f(\mathbf{w}^{(*)}))}{\eta \gamma \tau R} + \frac{L \eta \gamma (\omega + 1)}{k} \sigma^2 + L^2 \eta^2 \tau \sigma^2.$$

616 From the above inequality, is it easy to see that in order to achieve a linear speed up, we need to have

617 $\eta \gamma = O \left(\frac{\sqrt{k}}{\sqrt{R \tau}} \right).$ □

618 **Corollary 3** (Linear speed up). *In (14) for the choice of $\eta \gamma = O \left(\frac{1}{L} \sqrt{\frac{k}{R \tau (\omega + 1)}} \right)$, and $\gamma \geq k$ the
 619 convergence rate reduces to:*

$$\frac{1}{R} \sum_{r=0}^{R-1} \left\| \nabla f(\mathbf{w}^{(r)}) \right\|_2^2 \leq O \left(\frac{L \sqrt{(\omega + 1)} (f(\mathbf{w}^{(0)}) - f(\mathbf{w}^{*}))}{\sqrt{k R \tau}} + \frac{\left(\sqrt{(\omega + 1)} \right) \sigma^2}{\sqrt{k R \tau}} + \frac{k \sigma^2}{R \gamma^2} \right). \quad (19)$$

620 Note that according to (19), if we pick a fixed constant value for γ , in order to achieve an ϵ -accurate
 621 solution, $R = O\left(\frac{1}{\epsilon}\right)$ communication rounds and $\tau = O\left(\frac{\omega+1}{k\epsilon}\right)$ local updates are necessary. We
 622 also highlight that (19) also allows us to choose $R = O\left(\frac{\omega+1}{\epsilon}\right)$ and $\tau = O\left(\frac{1}{k\epsilon}\right)$ to get the same
 623 convergence rate.

624 **Remark 3.** Condition in (13) can be rewritten as

$$\begin{aligned}\eta &\leq \frac{-\gamma L\tau \left(\frac{\omega}{k} + 1\right) + \sqrt{\gamma^2 \left(L\tau \left(\frac{\omega}{k} + 1\right)\right)^2 + 4L^2\tau^2}}{2L^2\tau^2} \\ &= \frac{-\gamma L\tau \left(\frac{\omega}{k} + 1\right) + L\tau \sqrt{\left(\frac{\omega}{k} + 1\right)^2 \gamma^2 + 4}}{2L^2\tau^2} \\ &= \frac{\sqrt{\left(\frac{\omega}{k} + 1\right)^2 \gamma^2 + 4} - \left(\frac{\omega}{k} + 1\right) \gamma}{2L\tau}.\end{aligned}\quad (20)$$

625 So based on (20), if we set $\eta = O\left(\frac{1}{L\gamma} \sqrt{\frac{k}{R\tau(\omega+1)}}\right)$, it implies that:

$$R \geq \frac{\tau k}{(\omega + 1) \gamma^2 \left(\sqrt{\left(\frac{\omega}{k} + 1\right)^2 \gamma^2 + 4} - \left(\frac{\omega}{k} + 1\right) \gamma \right)^2}.\quad (21)$$

626 We note that $\gamma^2 \left(\sqrt{\left(\frac{\omega}{k} + 1\right)^2 \gamma^2 + 4} - \left(\frac{\omega}{k} + 1\right) \gamma \right)^2 = \Theta(1) \leq 5$ therefore even for $\gamma \geq m$ we
 627 need to have

$$R \geq \frac{\tau k}{5(\omega + 1)} = O\left(\frac{\tau k}{(\omega + 1)}\right).\quad (22)$$

628 Therefore, for the choice of $\tau = O\left(\frac{\omega+1}{k\epsilon}\right)$, due to condition in (22), we need to have $R = O\left(\frac{1}{\epsilon}\right)$.
 629 Similarly, we can have $R = O\left(\frac{\omega+1}{\epsilon}\right)$ and $\tau = O\left(\frac{1}{k\epsilon}\right)$.

630 **Corollary 4** (Special case, $\gamma = 1$). By letting $\gamma = 1$, $\omega = 0$ and $k = p$ the convergence rate in (14)
 631 reduces to

$$\frac{1}{R} \sum_{r=0}^{R-1} \left\| \nabla f(\mathbf{w}^{(r)}) \right\|_2^2 \leq \frac{2(f(\mathbf{w}^{(0)}) - f(\mathbf{w}^{(*)}))}{\eta R \tau} + \frac{L\eta}{p} \sigma^2 + L^2 \eta^2 \tau \sigma^2,$$

632 which matches the rate obtained in Wang and Joshi [43]. In this case the communication complexity
 633 and the number of local updates become

$$R = O\left(\frac{p}{\epsilon}\right), \quad \tau = O\left(\frac{1}{\epsilon}\right),$$

634 which simply implies that in this special case the convergence rate of our algorithm reduces to the
 635 rate obtained in Wang and Joshi [43], which indicates the tightness of our analysis.

636 C.1.2 Main result for the PL/Strongly convex setting

637 We now turn to stating the convergence rate for the homogeneous setting under PL condition which
 638 naturally leads to the same rate for strongly convex functions.

639 **Theorem 5** (PL or strongly convex). For $\text{FedSKETCH}(\tau, \eta, \gamma)$, for all $0 \leq t \leq R\tau - 1$, under
 640 Assumptions 1 to 2 and 3, if the learning rate satisfies

$$1 \geq \tau^2 L^2 \eta^2 + \left(\frac{\omega}{k} + 1\right) \eta \gamma L \tau$$

641 and if the all the models are initialized with $\mathbf{w}^{(0)}$ we obtain:

$$\mathbb{E} \left[f(\mathbf{w}^{(R)}) - f(\mathbf{w}^{(*)}) \right] \leq (1 - \eta \gamma \mu \tau)^R \left(f(\mathbf{w}^{(0)}) - f(\mathbf{w}^{(*)}) \right) + \frac{1}{\mu} \left[\frac{1}{2} L^2 \tau \eta^2 \sigma^2 + (1 + \omega) \frac{\gamma \eta L \sigma^2}{2k} \right]$$

642 *Proof.* From (18) under condition:

$$1 \geq \tau L^2 \eta^2 \tau + \left(\frac{\omega}{k} + 1\right) \eta \gamma L \tau$$

643 we obtain:

$$\begin{aligned} \mathbb{E} \left[f(\mathbf{w}^{(r+1)}) - f(\mathbf{w}^{(r)}) \right] &\leq -\eta \gamma \frac{\tau}{2} \left\| \nabla f(\mathbf{w}^{(r)}) \right\|_2^2 + \frac{L \tau \gamma \eta^2}{2k} (k L \tau \eta + \gamma(\omega + 1)) \sigma^2 \\ &\leq -\eta \mu \gamma \tau \left(f(\mathbf{w}^{(r)}) - f(\mathbf{w}^{(r)}) \right) + \frac{L \tau \gamma \eta^2}{2k} (k L \tau \eta + \gamma(\omega + 1)) \sigma^2 \end{aligned} \quad (23)$$

644 which leads to the following bound:

$$\mathbb{E} \left[f(\mathbf{w}^{(r+1)}) - f(\mathbf{w}^{(*)}) \right] \leq (1 - \eta \mu \gamma \tau) \left[f(\mathbf{w}^{(r)}) - f(\mathbf{w}^{(*)}) \right] + \frac{L \tau \gamma \eta^2}{2k} (k L \tau \eta + (\omega + 1) \gamma) \sigma^2$$

645 By setting $\Delta = 1 - \eta \mu \gamma \tau$ we obtain the following bound:

$$\begin{aligned} &\mathbb{E} \left[f(\mathbf{w}^{(R)}) - f(\mathbf{w}^{(*)}) \right] \\ &\leq \Delta^R \left[f(\mathbf{w}^{(0)}) - f(\mathbf{w}^{(*)}) \right] + \frac{1 - \Delta^R}{1 - \Delta} \frac{L \tau \gamma \eta^2}{2k} (k L \tau \eta + (\omega + 1) \gamma) \sigma^2 \\ &\leq \Delta^R \left[f(\mathbf{w}^{(0)}) - f(\mathbf{w}^{(*)}) \right] + \frac{1}{1 - \Delta} \frac{L \tau \gamma \eta^2}{2k} (k L \tau \eta + (\omega + 1) \gamma) \sigma^2 \\ &= (1 - \eta \mu \gamma \tau)^R \left[f(\mathbf{w}^{(0)}) - f(\mathbf{w}^{(*)}) \right] + \frac{1}{\eta \mu \gamma \tau} \frac{L \tau \gamma \eta^2}{2k} (k L \tau \eta + (\omega + 1) \gamma) \sigma^2 \end{aligned} \quad (24)$$

646

□

647 **Corollary 5.** If we let $\eta \gamma \mu \tau \leq \frac{1}{2}$, $\eta = \frac{1}{2L(\frac{\omega}{k} + 1)\tau \gamma}$ and $\kappa = \frac{L}{\mu}$ the convergence error in Theorem 5,

648 with $\gamma \geq k$ results in:

$$\begin{aligned} &\mathbb{E} \left[f(\mathbf{w}^{(R)}) - f(\mathbf{w}^{(*)}) \right] \\ &\leq e^{-\eta \gamma \mu \tau R} \left(f(\mathbf{w}^{(0)}) - f(\mathbf{w}^{(*)}) \right) + \frac{1}{\mu} \left[\frac{1}{2} \tau L^2 \eta^2 \sigma^2 + (1 + \omega) \frac{\gamma \eta L \sigma^2}{2k} \right] \\ &\leq e^{-\frac{R}{2(\frac{\omega}{k} + 1)\kappa}} \left(f(\mathbf{w}^{(0)}) - f(\mathbf{w}^{(*)}) \right) + \frac{1}{\mu} \left[\frac{1}{2} L^2 \frac{\tau \sigma^2}{L^2 (\frac{\omega}{k} + 1)^2 \gamma^2 \tau^2} + \frac{(1 + \omega) L \sigma^2}{2 (\frac{\omega}{k} + 1) L \tau k} \right] \\ &= O \left(e^{-\frac{R}{2(\frac{\omega}{k} + 1)\kappa}} \left(f(\mathbf{w}^{(0)}) - f(\mathbf{w}^{(*)}) \right) + \frac{\sigma^2}{(\frac{\omega}{k} + 1)^2 \gamma^2 \mu \tau} + \frac{(\omega + 1) \sigma^2}{\mu (\frac{\omega}{k} + 1) \tau k} \right) \\ &= O \left(e^{-\frac{R}{2(\frac{\omega}{k} + 1)\kappa}} \left(f(\mathbf{w}^{(0)}) - f(\mathbf{w}^{(*)}) \right) + \frac{\sigma^2}{\gamma^2 \mu \tau} + \frac{(\omega + 1) \sigma^2}{\mu (\frac{\omega}{k} + 1) \tau k} \right) \end{aligned} \quad (25)$$

649 which indicates that to achieve an error of ϵ , we need to have $R = O \left(\left(\frac{\omega}{k} + 1 \right) \kappa \log \left(\frac{1}{\epsilon} \right) \right)$ and $\tau =$
 650 $\frac{(\omega + 1)}{k(\frac{\omega}{k} + 1)\epsilon}$. Additionally, we note that if $\gamma \rightarrow \infty$, yet $R = O \left(\left(\frac{\omega}{k} + 1 \right) \kappa \log \left(\frac{1}{\epsilon} \right) \right)$ and $\tau = \frac{(\omega + 1)}{k(\frac{\omega}{k} + 1)\epsilon}$
 651 will be necessary.

652 C.1.3 Main result for the general convex setting

653 **Theorem 6 (Convex).** For a general convex function $f(\mathbf{w})$ with optimal solution $\mathbf{w}^{(*)}$, using
 654 *FedSKETCH*(τ, η, γ) to optimize $\hat{f}(\mathbf{w}, \phi) = f(\mathbf{w}) + \frac{\phi}{2} \|\mathbf{w}\|^2$, for all $0 \leq t \leq R\tau - 1$, under
 655 Assumptions 1 to 2, if the learning rate satisfies

$$1 \geq \tau^2 L^2 \eta^2 + \left(\frac{\omega}{k} + 1\right) \eta \gamma L \tau$$

656 and if the all the models initiate with $\mathbf{w}^{(0)}$, with $\phi = \frac{1}{\sqrt{k\tau}}$ and $\eta = \frac{1}{2L\gamma\tau(1+\frac{\omega}{k})}$ we obtain:

$$\begin{aligned} \mathbb{E}\left[f(\mathbf{w}^{(R)}) - f(\mathbf{w}^{(*)})\right] &\leq e^{-\frac{R}{2L(1+\frac{\omega}{k})\sqrt{m\tau}}} \left(f(\mathbf{w}^{(0)}) - f(\mathbf{w}^{(*)})\right) \\ &\quad + \left[\frac{\sqrt{k}\sigma^2}{8\sqrt{\tau}\gamma^2(1+\frac{\omega}{k})^2} + \frac{(\omega+1)\sigma^2}{4(\frac{\omega}{k}+1)\sqrt{k\tau}}\right] + \frac{1}{2\sqrt{k\tau}} \|\mathbf{w}^{(*)}\|^2 \end{aligned} \quad (26)$$

657 We note that above theorem implies that to achieve a convergence error of ϵ we need to have
 658 $R = O\left(L\left(1+\frac{\omega}{k}\right)\frac{1}{\epsilon}\log\left(\frac{1}{\epsilon}\right)\right)$ and $\tau = O\left(\frac{(\omega+1)^2}{k(\frac{\omega}{k}+1)^2\epsilon}\right)$.

659 *Proof.* Since $\tilde{f}(\mathbf{w}^{(r)}, \phi) = f(\mathbf{w}^{(r)}) + \frac{\phi}{2} \|\mathbf{w}^{(r)}\|^2$ is ϕ -PL, according to Theorem 5, we have:

$$\begin{aligned} &\tilde{f}(\mathbf{w}^{(R)}, \phi) - \tilde{f}(\mathbf{w}^{(*)}, \phi) \\ &= f(\mathbf{w}^{(r)}) + \frac{\phi}{2} \|\mathbf{w}^{(r)}\|^2 - \left(f(\mathbf{w}^{(*)}) + \frac{\phi}{2} \|\mathbf{w}^{(*)}\|^2\right) \\ &\leq (1 - \eta\gamma\phi\tau)^R \left(f(\mathbf{w}^{(0)}) - f(\mathbf{w}^{(*)})\right) + \frac{1}{\phi} \left[\frac{1}{2}L^2\tau\eta^2\sigma^2 + (1+\omega)\frac{\gamma\eta L\sigma^2}{2k}\right] \end{aligned} \quad (27)$$

660 Next rearranging (27) and replacing μ with ϕ leads to the following error bound:

$$\begin{aligned} &f(\mathbf{w}^{(R)}) - f^* \\ &\leq (1 - \eta\gamma\phi\tau)^R \left(f(\mathbf{w}^{(0)}) - f(\mathbf{w}^{(*)})\right) + \frac{1}{\phi} \left[\frac{1}{2}L^2\tau\eta^2\sigma^2 + (1+\omega)\frac{\gamma\eta L\sigma^2}{2k}\right] \\ &\quad + \frac{\phi}{2} \left(\|\mathbf{w}^*\|^2 - \|\mathbf{w}^{(r)}\|^2\right) \\ &\leq e^{-(\eta\gamma\phi\tau)R} \left(f(\mathbf{w}^{(0)}) - f(\mathbf{w}^{(*)})\right) + \frac{1}{\phi} \left[\frac{1}{2}L^2\tau\eta^2\sigma^2 + (1+\omega)\frac{\gamma\eta L\sigma^2}{2k}\right] + \frac{\phi}{2} \|\mathbf{w}^{(*)}\|^2 \end{aligned}$$

661 Next, if we set $\phi = \frac{1}{\sqrt{k\tau}}$ and $\eta = \frac{1}{2(1+\frac{\omega}{k})L\gamma\tau}$, we obtain that

$$\begin{aligned} &f(\mathbf{w}^{(R)}) - f^* \\ &\leq e^{-\frac{R}{2(1+\frac{\omega}{k})L\sqrt{m\tau}}} \left(f(\mathbf{w}^{(0)}) - f(\mathbf{w}^{(*)})\right) + \sqrt{k\tau} \left[\frac{\sigma^2}{8\tau\gamma^2(1+\frac{\omega}{k})^2} + \frac{(\omega+1)\sigma^2}{4(\frac{\omega}{k}+1)\tau k}\right] + \frac{1}{2\sqrt{k\tau}} \|\mathbf{w}^{(*)}\|^2, \end{aligned}$$

662 thus the proof is complete. \square

C.2 Proof of Theorem 2

The proof of Theorem 2 follows directly from the results in Haddadpour et al. [13]. We first mention the general Theorem 7 from [13] for general compression noise ω . Next, since the sketching PRIVIX and HEAPRIX, satisfy Assumption 4 with $\omega = c\frac{d}{m}$ and $\omega = c\frac{d}{m} - 1$ respectively with probability $1 - \frac{\delta}{R}$ per communication round, all the results in Theorem 2, conclude from Theorem 7 with probability $1 - \delta$ (by taking union over the all probabilities of each communication rounds with probability $1 - \delta/R$) and plugging $\omega = c\frac{d}{m}$ and $\omega = c\frac{d}{m} - 1$ respectively into the corresponding convergence bounds. For the heterogeneous setting, the results in Haddadpour et al. [13] requires the following extra assumption that naturally holds for the sketching:

Assumption 5 (Haddadpour et al. [13]). *The compression scheme Q for the heterogeneous data distribution setting satisfies the following condition $\mathbb{E}_Q[\|\frac{1}{m} \sum_{j=1}^m Q(\mathbf{x}_j)\|^2 - \|Q(\frac{1}{m} \sum_{j=1}^m \mathbf{x}_j)\|^2] \leq G_q$.*

We note that since sketching is a linear compressor, in the case of our algorithms for heterogeneous setting we have $G_q = 0$.

Next, we restate the Theorem in Haddadpour et al. [13] here as follows:

Theorem 7. *Consider FedCOMGATE in Haddadpour et al. [13]. If Assumptions 1, 3, 4 and 5 hold, then even for the case the local data distribution of users are different (heterogeneous setting) we have*

- **non-convex:** By choosing stepsizes as $\eta = \frac{1}{L\gamma} \sqrt{\frac{p}{R\tau(\omega+1)}}$ and $\gamma \geq p$, we obtain that the iterates satisfy $\frac{1}{R} \sum_{r=0}^{R-1} \|\nabla f(\mathbf{w}^{(r)})\|_2^2 \leq \epsilon$ if we set $R = O\left(\frac{\omega+1}{\epsilon}\right)$ and $\tau = O\left(\frac{1}{p\epsilon}\right)$.
- **Strongly convex or PL:** By choosing stepsizes as $\eta = \frac{1}{2L(\frac{\omega}{p}+1)\tau\gamma}$ and $\gamma \geq \sqrt{p\tau}$, we obtain that the iterates satisfy $\mathbb{E}[f(\mathbf{w}^{(R)}) - f(\mathbf{w}^{(*)})] \leq \epsilon$ if we set $R = O\left((\omega+1)\kappa \log\left(\frac{1}{\epsilon}\right)\right)$ and $\tau = O\left(\frac{1}{p\epsilon}\right)$.
- **Convex:** By choosing stepsizes as $\eta = \frac{1}{2L(\omega+1)\tau\gamma}$ and $\gamma \geq \sqrt{p\tau}$, we obtain that the iterates satisfy $\mathbb{E}[f(\mathbf{w}^{(R)}) - f(\mathbf{w}^{(*)})] \leq \epsilon$ if we set $R = O\left(\frac{L(1+\omega)}{\epsilon} \log\left(\frac{1}{\epsilon}\right)\right)$ and $\tau = O\left(\frac{1}{p\epsilon^2}\right)$.

Proof. Since the sketching methods PRIVIX and HEAPRIX, satisfy the Assumption 4 with $\omega = c\frac{d}{m}$ and $\omega = c\frac{d}{m} - 1$ respectively with probability $1 - \frac{\delta}{R}$ per communication round, we conclude the proofs of Theorem 2 using Theorem 7 with probability $1 - \delta$ (by taking union over all communication rounds) and plugging $\omega = c\frac{d}{m}$ and $\omega = c\frac{d}{m} - 1$ respectively into the convergence bounds. \square

D Numerical Experiments and Additional Results

D.1 Implementation of FetchSGD

Our implementation of FetchSGD basically follows the original paper (Algorithm 1 in [37]). The only difference is that, in the original algorithm, the local workers compress the gradient (in every local step) and transmit it to the central server. In our setting, we extend to the case with multiple local updates, where the difference in local weights are transmitted (same as the standard FL framework). Also, TopK compression is used to decode the sketches at the central server. We apply the same

699 implementation trick that when accumulating the errors, we only count the non-zero coordinates and
700 leave other coordinates zero for the accumulator. This greatly improves the empirical performance.

701 D.2 Additional Plots for the MNIST Experiments

702 D.2.1 Homogeneous setting

703 In the homogeneous case, each node has same data distribution. To achieve this setting, we randomly
 704 choose samples uniformly from 10 classes of hand-written digits. The train loss and test accuracy
 705 are provided in Figure 3, where we report local epochs $\tau = 2$ in addition to the main context (single
 706 local update). The number of users is set to 50, and in each round of training we randomly pick half
 707 of the nodes to be active (i.e., receiving data and performing local updates). We can draw similar
 708 conclusion: FS-HEAPRIX consistently performs better than other competing methods. The test
 709 accuracy increases with larger τ in homogeneous setting.

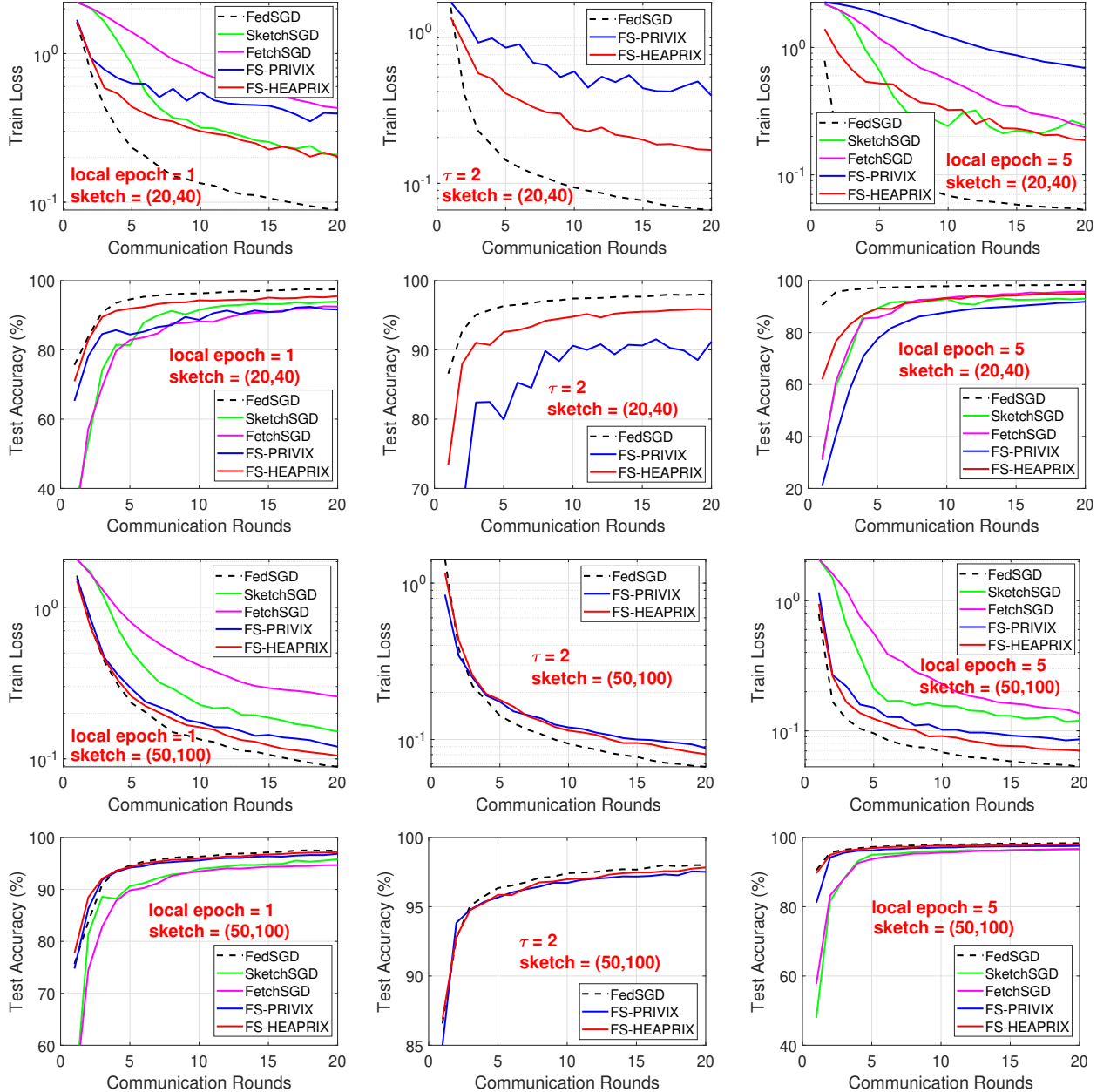


Figure 3: MNIST Homogeneous case: Comparison of compressed optimization methods on LeNet CNN architecture.

710 D.2.2 Heterogeneous setting

711 Analogously, we present experiments on MNIST dataset under heterogeneous data distribution,
 712 including $\tau = 2$. We simulate the setting by only sending samples from one digit to each local
 713 worker (very few nodes get two classes). We see from Figure 4 that FS-HEAPRIX shows consistent
 714 advantage over competing methods. SketchedSGD performs poorly in this case.

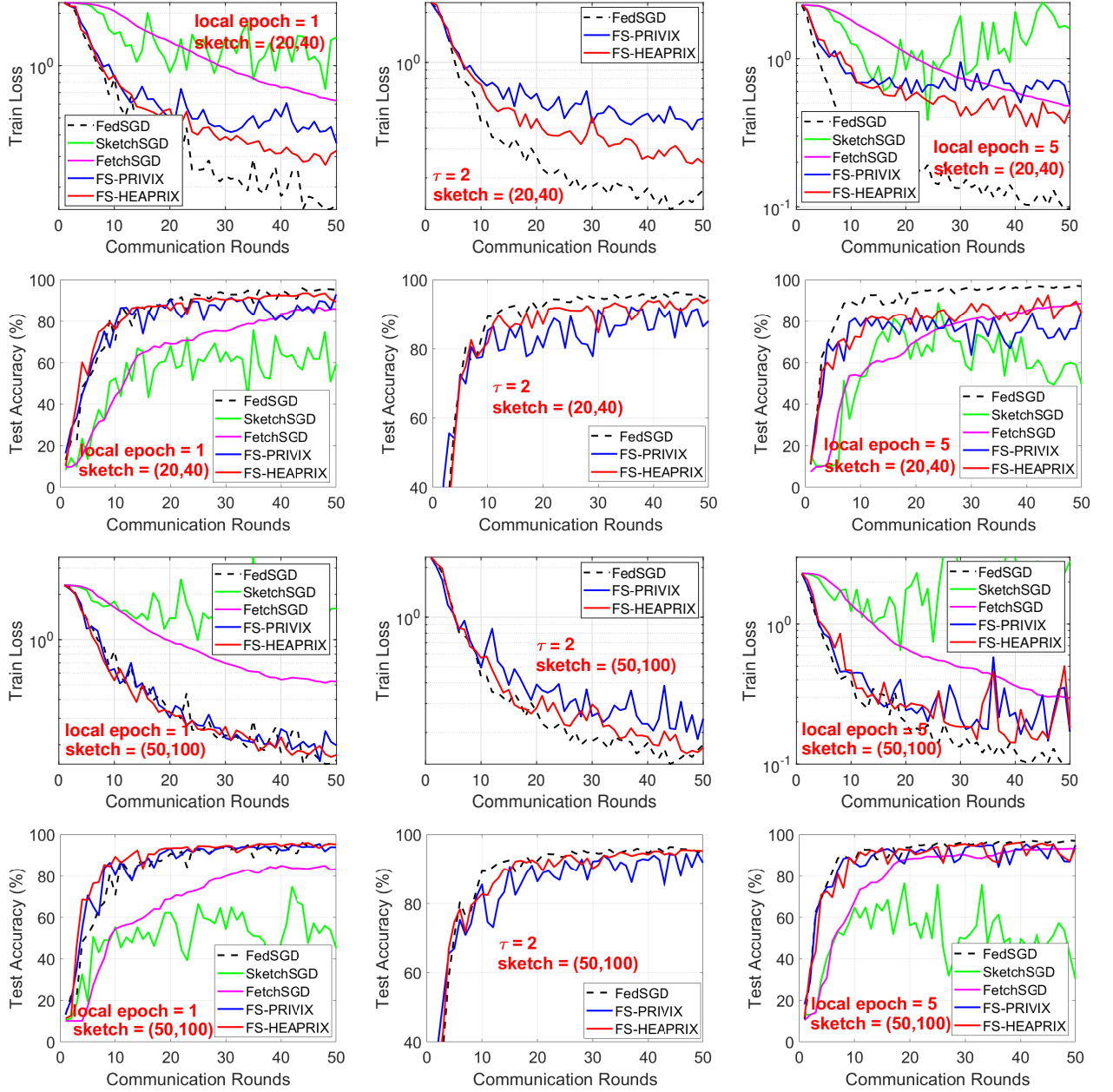


Figure 4: MNIST Heterogeneous case: Comparison of compressed optimization algorithms on LeNet CNN architecture.

715 D.3 Additional Experiments: CIFAR-10

716 We conduct similar sets of experiments on CIFAR10 dataset. We also use the simple LeNet CNN
 717 structure, as in practice small models are more favorable in federated learning, due to the limitation of
 718 mobile devices. The test accuracy is presented in Figure 5 and Figure 6, for respectively homogeneous
 719 and heterogeneous data distribution. In general, we retrieve similar information as from MNIST
 720 experiments: our proposed FS-HEAPRIX improves FS-PRIVIX and SketchedSGD in all cases. We
 721 note that although the test accuracy provided by LeNet cannot reach the state-of-the-art accuracy
 722 given by some huge models, it is also informative in terms of comparing the relative performance of
 723 different sketching methods.

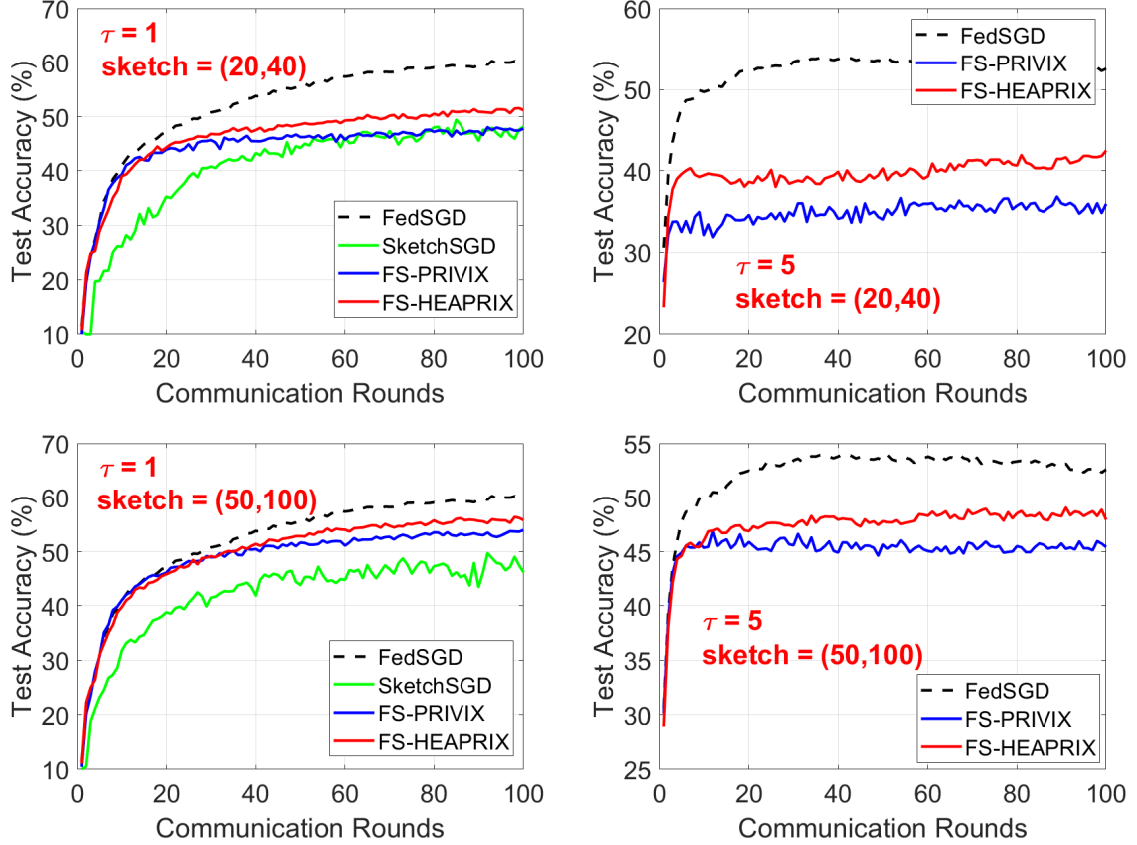


Figure 5: Homogeneous case: CIFAR10: Comparison of compressed optimization methods on LeNet CNN.

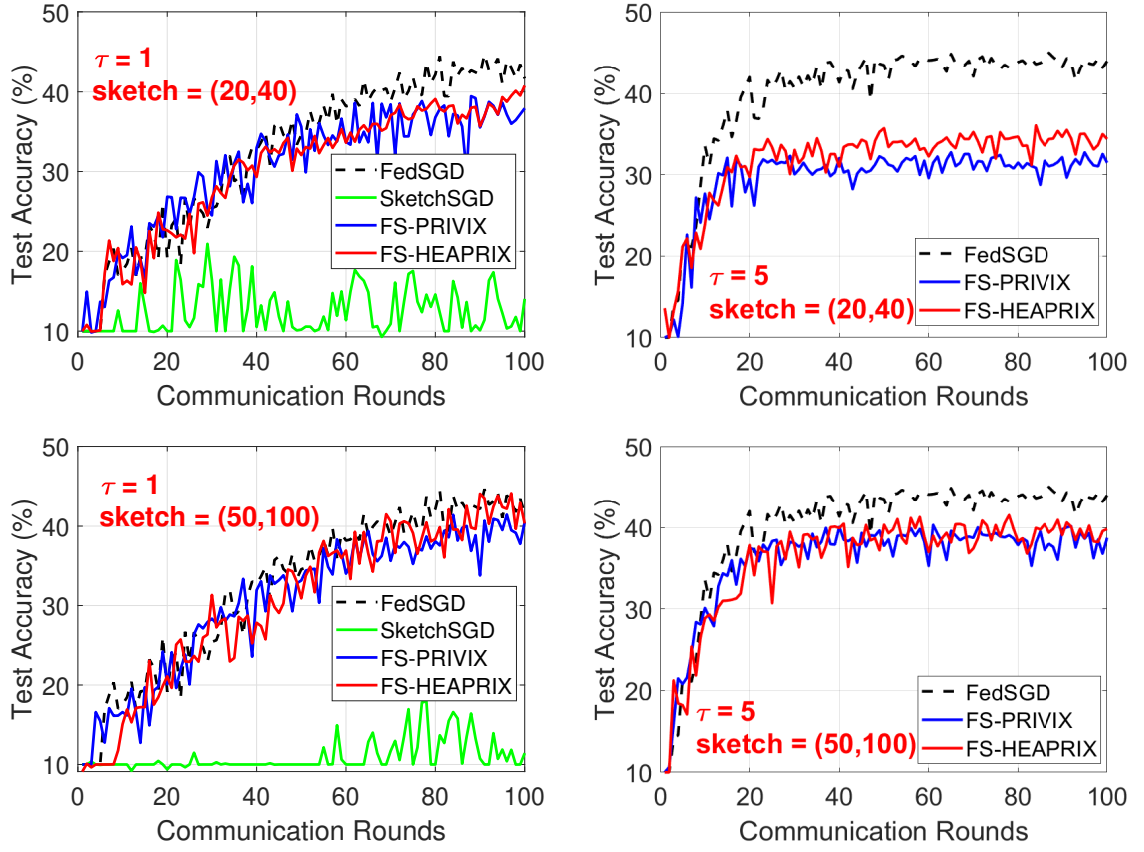


Figure 6: Heterogeneous case: CIFAR10: Comparison of compressed optimization methods on LeNet CNN.